

See discussions, stats, and author profiles for this publication at: <https://www.researchgate.net/publication/394544740>

Volcano–Tectonic Controls on Magmatic Evolution at Campi Flegrei, Italy: Insights from Thermodynamic Modelling

Article in *Journal of Petrology* · July 2025

DOI: 10.1093/petrology/egaf068

CITATION

1

READS

60

7 authors, including:



Michael Stock

Trinity College Dublin

53 PUBLICATIONS 1,087 CITATIONS

[SEE PROFILE](#)



Victoria C. Smith

University of Oxford

183 PUBLICATIONS 6,894 CITATIONS

[SEE PROFILE](#)



Roberto Isaia

Istituto Nazionale di Geofisica e Vulcanologia

197 PUBLICATIONS 7,161 CITATIONS

[SEE PROFILE](#)



Stefano Vitale

University of Naples Federico II

204 PUBLICATIONS 3,641 CITATIONS

[SEE PROFILE](#)

Volcano-Tectonic Controls on Magmatic Evolution at Campi Flegrei, Italy: Insights from Thermodynamic Modelling

FAY M. AMSTUTZ¹, MICHAEL J. STOCK¹, VICTORIA C. SMITH², ROBERTO ISAIA³, STEFANO VITALE⁴, ELLIOT J. CARTER^{1,5} and JACOPO NATALE⁶

¹Discipline of Geology, Museum Building, Trinity College Dublin, Dublin, D02 PN40, Ireland

²Research Laboratory for Archaeology and the History of Art, Dyson Perrins Building, South Parks Road, University of Oxford, Oxford, OX1 3TG, UK

³Istituto Nazionale di Geofisica e Vulcanologia, Osservatorio Vesuviano, via Diocleziano 328, 80124 Napoli, Italy

⁴Dipartimento di Scienze della Terra, dell'Ambiente e delle Risorse (DiSTAR), Università di Napoli Federico II, Via Vicinale Cupa Cintia 21, 80126 Napoli, Italy

⁵School of Life Sciences, Huxley Building, Keele University, Staffordshire, ST5 5BG, UK

⁶Dipartimento di Scienze della Terra e Geoambientali, Università degli Studi di Bari Aldo Moro, Via Orabona, 4, 70125 Bari, Italy

*Corresponding author. Telephone: +353 1 896 1074, E-mail: amstutzf@tcd.ie

Campi Flegrei caldera (Naples, southern Italy) is one of the most hazardous volcanoes on Earth, having produced >70 eruptions in the past 15 kyr, and currently showing significant signs of unrest within a densely populated part of Europe. Post-15 ka eruptions span a range of eruptive styles and compositions, which broadly correlate with the spatial and structural location of vents within the large caldera: eruptions from vents along the northern and eastern caldera rim faults are typically small and extend to mafic compositions; eruptions from vents in the central and eastern side of the caldera extend to evolved compositions and have produced Plinian columns; and vents along regional faults (also activated by caldera collapse) in the western caldera have produced sub-Plinian eruptions, which are often relatively Na₂O-rich and K₂O-depleted. These compositional and eruptive differences suggest an intrinsic link between their volcano-tectonic setting and structure and/or processes operating within the sub-volcanic magmatic system. To investigate this, we compare post-15 ka erupted glass major element compositions to liquid lines of descent produced using the rhyolite-MELTS thermodynamic model. To constrain magma storage conditions at Campi Flegrei, we systematically vary the crystallisation conditions in 1800 models before employing a new statistical approach to assess the quality of fit between natural glass compositions and model outputs. In simple (uncontaminated) fractional crystallisation models, we find that glass compositions in each volcano-tectonic setting are best reproduced by similar storage conditions: pressure of 110–160 MPa, liquidus oxygen fugacity of 0–1 log unit above the quartz–fayalite–magnetite buffer, and a liquidus H₂O concentration of 2 wt % for the northern, eastern and western caldera eruptions and 3 wt % for the central caldera eruptions. However, the addition of an assimilant further improves the fit between predicted and observed major element compositions, with the amount and type of assimilant varying between volcano-tectonic settings. Best-fit models for vents along the northern and eastern caldera rim faults include small (5–10%) amounts of Palaeozoic metamorphic basement, whereas those for vents in the centre of the caldera or along the western regional faults include larger quantities (~30%) of assimilated syenitic restite. The Fondi di Baia eruption is compositionally anomalous, and its evolution may reflect minor limestone or hydrothermal calcite contamination. Our results demonstrate a novel link between the spatial and structural location of vents within the Campi Flegrei caldera and the physicochemical processes operating within its magmatic system, providing important information for the assessment of future hazard scenarios.

Key words: assimilation; Campi Flegrei; fractional crystallisation; rhyolite-MELTS modelling; volcano-tectonic control

INTRODUCTION

Caldera-forming volcanoes occur worldwide and are frequently associated with long-lived magmatic systems, which produce eruptions of varying size, style and composition through time (Cole *et al.*, 2005). Following collapse, post-caldera eruptions typically occur in different spatial locations across the volcanic system, including along caldera ring faults and regional lineaments (Lipman, 1984); vent locations are often directly related to local volcano-tectonic structures, with magma ascent exploiting

pre-existing planes of weakness (Robertson *et al.*, 2016; Németh *et al.*, 2017; Pérez-Orozco *et al.*, 2021). Compositional variations in erupted products are controlled by complex processes operating within the sub-volcanic crustal magma system, in addition to mantle heterogeneity (Pearce & Peate, 1995; Annen *et al.*, 2015), with the major element variations controlling magma rheology and chemical properties (e.g. viscosity and volatile solubility), which in turn impact the timing and style of eruptions (Cassidy *et al.*, 2018). However, the relationship between volcano-tectonic structures and sub-volcanic processes is poorly understood; it

RECEIVED NOVEMBER 6, 2024; REVISED JULY 14, 2025; ACCEPTED JULY 23, 2025

© The Author(s) 2025. Published by Oxford University Press.

This is an Open Access article distributed under the terms of the Creative Commons Attribution License (<https://creativecommons.org/licenses/by/4.0/>), which permits unrestricted reuse, distribution, and reproduction in any medium, provided the original work is properly cited.

remains unclear whether structural controls can impact the dynamics of magmatic systems and compositions of erupted melts. Addressing this has important implications for hazard assessment and the interpretation of monitoring data where unrest in different parts of a large active caldera system might reflect different crustal processes and result in different volcanic eruption styles or compositions.

Campi Flegrei volcano (southern Italy) has produced >70 eruptions since the last major caldera collapse at 15 ka (the Neapolitan Yellow Tuff [NYT] eruption; Smith *et al.*, 2011). While the primary mantle melts feeding these post-15 ka eruptions are thought to be relatively constant with respect to the major element composition (Mazzeo *et al.*, 2014), the distribution of vents is closely associated with regional structures (Peccerillo & Frezzotti, 2015; Peccerillo, 2017) and subtle variations in erupted compositions have been identified across the caldera system (D'Antonio *et al.*, 1999; Di Renzo *et al.*, 2011; Smith *et al.*, 2011). Hence, Campi Flegrei presents an ideal location to explore whether the volcano-tectonic setting of an eruption impacts processes operating within the sub-volcanic system. Additionally, the region around Campi Flegrei is densely populated (~1.5 million people living within the caldera, and more than ~3.5 million likely to be immediately impacted by an eruption) and the system is currently showing significant signs of unrest, making it one of the most hazardous volcanoes on Earth (Orsi *et al.*, 2004; Bevilacqua *et al.*, 2017). Constraining the magmatic processes that influence erupted compositions in different parts of the caldera system has important implications for hazard forecasting and the interpretation of volcano monitoring data.

Magma storage conditions can be determined in different volcanic environments using a variety of petrological methods. These include thermobarometry, using the pressure sensitivity of exchange reactions of chemical components between various mineral assemblages (Putirka, 2008); comparisons between the chemistry of erupted products and those from experiments conducted under controlled conditions (Blundy & Cashman, 2008); and saturation depths calculated from the volatile contents of melt inclusions (Anderson *et al.*, 1989). The influence of assimilation on magmatic evolution can also be investigated, for example by comparison of the isotopic composition of the magma and potential crustal contaminants (James, 1981). Previous studies have attempted to link storage conditions to volcano-tectonic setting across a caldera system, for example Saxby *et al.* (2016) demonstrated a link between regional fault patterns and location of magma storage at Ilopango caldera (El Salvador) on the basis of gravity surveys, whereas Carracedo *et al.* (2007) noted compositional variation of eruptions in different locations across Tenerife (Canary Islands). However, these techniques generally only allow assessment of magma storage conditions over discrete ranges in the evolution of the sub-volcanic system (i.e. within the crystallisation interval of the phase used in barometry) and typically provide information on one intrinsic variable (such as pressure for barometry or extent of assimilation for isotope mixing models). In this study, we use thermodynamic modelling to assess the range of variables which control magma storage conditions through the entire liquid line of descent, finding combinations of variables that are consistent with erupted compositions.

The rhyolite-MELTS thermodynamic modelling software calculates the stable phase assemblage in a magmatic system under given conditions, and can be applied to determine the evolving phase assemblage and phase compositions during fractional crystallisation (FC) or assimilation-fractional crystallisation (AFC, Gualda *et al.*, 2012; Ghiorso & Gualda, 2015).

Through systematically varying model crystallisation conditions (i.e. pressure, oxygen fugacity, initial melt major or volatile element composition) and comparing with the abundance and composition of phases in natural erupted materials, previous studies have successfully used rhyolite-MELTS (or its predecessor MELTS, which differs in the stability fields of quartz and sanidine, Ghiorso & Sack, 1995) outputs to constrain magma storage conditions in diverse volcanic systems (e.g. Peach Spring—Pamukcu *et al.*, 2015; Aluto—Gleeson *et al.*, 2017; individual Campi Flegrei eruptions—Fowler *et al.*, 2007; Fowler & Spera, 2010; Cannatelli, 2012). In general, these studies have identified the most probable set of magma storage conditions by visually identifying the modelled liquid line of descent, which best-fits erupted melt compositions. However, Gleeson *et al.* (2017) proposed a statistical method to quantify the fit between natural and predicted compositions, more accurately identifying the best set of model parameters where liquid lines of descent are similar or deviate from natural compositions over a limited (~30 °C) crystallisation interval.

Here, we use rhyolite-MELTS to model isobaric FC and AFC of a near-primitive Campi Flegrei liquid under different storage conditions, comparing the predicted phase assemblages and liquid lines of descent with erupted products from vents in different volcano-tectonic settings within the caldera. This extends previous work constraining magma storage for individual Campi Flegrei eruptions using MELTS modelling (e.g. Campanian Ignimbrite—Fowler *et al.*, 2007, Fowler & Spera, 2010; Minopoli 1 and Fondo Riccio—Cannatelli, 2012), investigating eruptions in the last 15 kyr for which there is published glass major element compositional data ($n = 48$). By systematically varying the model pressure (P), liquidus f_{O_2} ($L_{f_{\text{O}_2}}$), liquidus H_2O content ($L_{\text{H}_2\text{O}}$) and amount/type of assimilated material across the range of potential parameter space, we are able to constrain the conditions and processes operating during pre-eruptive magma storage, exploring the hypothesis that volcano-tectonic setting impacts magmatic evolution. As different combinations of storage conditions can produce model outputs that appear similar to a first order, we apply a novel statistical approach to assess the correlation between modelled liquid lines of descent and measured glass major element compositions. Our best-fit models (i.e. closest correlation between modelled liquid line of descent and natural glasses) are for magma storage conditions which agree well with previous estimates and show only minor variations between different volcano-tectonic settings. However, we find that the addition of assimilants ubiquitously improves the model fit, but that the type and amount of assimilant varies between eruptions from vents in different parts of the Campi Flegrei caldera, indicating spatial variations in the nature of magma-country rock interaction.

GEOLOGICAL SETTING

Campi Flegrei is the largest centre in the Phlegraean Volcanic District, an area of volcanism in southern Italy (near Naples; Orsi *et al.*, 1996), formed as a result of back arc extension and the opening the Tyrrhenian Sea, related to rollback of the subducting Ionian plate (Faccenna *et al.*, 2007; Peccerillo & Frezzotti, 2015). Large-scale tectonic deformation in the Phlegraean area has given rise to two main regional fault systems, trending NE–SW and NW–SE (Acocella, 2010; Vitale & Isaia, 2014), which have influenced both the distribution of vents (Bevilacqua *et al.*, 2015) and orientation of Campi Flegrei caldera collapse scarps (Orsi *et al.*, 1996; Di Vito *et al.*, 1999; Vitale & Isaia, 2014; Natale *et al.*, 2022a).

The oldest volcanism at Campi Flegrei is dated to >300 ka (De Vivo *et al.*, 2001; Rolandi *et al.*, 2003; Di Vito *et al.*, 2008; Fernandez *et al.*, 2024), with the eruptive history punctuated by at least three major caldera collapse events: the ~40 ka Campanian Ignimbrite (CI, Giaccio *et al.*, 2017), the ~29 ka Masseira del Monte Tuff (Albert *et al.*, 2019) and the ~15 ka NYT (Deino *et al.*, 2004). These eruptions have produced a nested caldera structure (~13 km diameter), with collapse scarps juxtaposed against the regional tectonic lineaments (Vitale & Isaia, 2014; Natale *et al.*, 2022a). In the past 15 kyr, Campi Flegrei has produced >70 eruptions from vents located within the NYT caldera (Di Vito *et al.*, 1999; Smith *et al.*, 2011), coupled with ground deformation (Isaia *et al.*, 2019; Natale *et al.*, 2022b). These can be broadly divided into three epochs of intense activity (mean eruption frequency 50–70 years), separated by periods of quiescence (~1–3.6 ka; Di Vito *et al.*, 1999): Epoch 1 produced ~30 magmatic and phreatomagmatic eruptions between ~15 and 10.6 ka; Epoch 2 produced 8 low magnitude eruptions between ~9.6 and 9.1 ka; and Epoch 3 produced 28 eruptions between ~5.5 to 3.5 ka. These eruptions display a range in eruptive style and magnitude from effusive lava domes, through small explosive events to the Plinian Agnano–Monte Spina eruption (de Vita *et al.*, 1999; Di Vito *et al.*, 1999; Smith *et al.*, 2011). The most recent Campi Flegrei eruption was at Monte Nuovo in 1538 CE, which is post-Epoch 3 and considered separate due to the long repose period between this event and the last eruption of Epoch 3 (>3 kyr, Piochi *et al.*, 2005; Smith *et al.*, 2011).

Vent locations for post-15 ka eruptions span the NYT caldera (Fig. 1) and can be broadly divided into three distinct volcano-tectonic settings: (1) those along caldera rim faults in the northern and eastern sectors of the caldera, which were either formed or reactivated during the NYT collapse and strike obliquely to the regional lineaments ('northern/eastern caldera eruptions'); (2) those in the west of the caldera aligned with caldera rim faults and regional tectonic fault systems characterised by a different orientation pattern of faults and fractures compared to those in the eastern sector ('western caldera eruptions'; Vitale & Isaia, 2014); and (3) those within the central caldera, which are not located along major pre-existing planes of crustal weakness ('central caldera eruptions'; Fig. 1; Di Vito *et al.*, 1999; Isaia *et al.*, 2009; Bevilacqua *et al.*, 2015; Natale *et al.*, 2022b). Differences in the frequency and composition of eruptions as well as structural differences in fault patterns between the east and west of the caldera has led other authors to make similar divisions (Vilardo *et al.*, 2010; Vitale & Isaia, 2014; Bevilacqua *et al.*, 2016, 2017). In general, earlier eruptions were fed by magmas that exploited the caldera rim faults (including regional fault systems reactivated during caldera collapse), with later eruptions migrating towards the caldera interior (particularly in the northeastern sector; Di Vito *et al.*, 1999; Isaia *et al.*, 2009) or regional tectonic faults in the western caldera (Di Vito *et al.*, 1999; Vilardo *et al.*, 2010; Vitale & Isaia, 2014).

Throughout its history, Campi Flegrei has consistently produced alkali magmas (Vineberg *et al.*, 2023), with melts of the post-15 ka eruptions ranging from shoshonite to phonolite in composition (Smith *et al.*, 2011). Magmas do not form a continual compositional trend between eruptive periods, but the most mafic shoshonitic products are from Epoch 1 with later eruptions extending to more evolved phonolite to trachyte compositions (Smith *et al.*, 2011). Several previous studies have noted a correlation between the volcano-tectonic setting of eruption vents and the composition of erupted products (D'Antonio *et al.*, 1999; Di Renzo *et al.*, 2011; Smith *et al.*, 2011). In general, the northern/eastern caldera eruptions are the most primitive, occurring from

NYT caldera rim faults (Civetta *et al.*, 1991) with more evolved Epoch 2 and Epoch 3 eruptions from the northeastern caldera floor, and their products are indistinguishable on the basis of major element chemistry (Smith *et al.*, 2011). Eruptions from vents in the west of the caldera have been noted as the most compositionally diverse; for example, the Baia-Fondi di Baia deposits are highly evolved with distinct trace element concentrations relative to other post-15 ka eruptions (Smith *et al.*, 2011; Voloschina *et al.*, 2018).

Previous studies generally agree on the architecture of the Campi Flegrei sub-volcanic system being characterised by a main magma storage zone at ~7–8 km depth, with shallow (possibly ephemeral) sills at around 3–4 km depth (Stock *et al.*, 2018; Petrelli *et al.*, 2023). Seismic tomography and magnetotelluric investigations have imaged a main region of magma storage at ~7.5 km (Zollo *et al.*, 2008; Bianco *et al.*, 2022; Isaia *et al.*, 2025) and small shallow reservoirs between 2 and 4 km (De Siena *et al.*, 2010; Calò & Tramelli, 2018; Giacomuzzi *et al.*, 2024). This agrees with pressures obtained from the volatile contents of melt inclusions, which give saturation depths of ~2 to ~9 km for multiple eruptions in the last 15 kyr (Mangiacapra *et al.*, 2008; Arienzo *et al.*, 2010, 2016; Vetere *et al.*, 2011; Fourmentraux *et al.*, 2012; Voloschina *et al.*, 2018). Thermobarometry estimates of crystallisation depth suggest a main region of magma storage around 8 km (Astbury *et al.*, 2018; Giordano & Caricchi, 2022), with slightly shallower estimates of ~3–6 km from chlorine geobarometry (Balcone-Boissard *et al.*, 2024). Previous phase equilibria investigations at Campi Flegrei found observed compositions best reproduced by crystallisation depths of 6–12 km for the CI and two post-15 ka eruptions (Minopoli 1 and Fondo Riccio; Bohron *et al.*, 2006; Fowler *et al.*, 2007; Cannatelli, 2012). Measurements in melt inclusions from various eruptions agree on H₂O contents of 0.8–6% (Webster *et al.*, 2003; Cannatelli *et al.*, 2007; Mangiacapra *et al.*, 2008; Arienzo *et al.*, 2010, 2016; Fourmentraux *et al.*, 2012; Stock *et al.*, 2018), in agreement with estimates from K-feldspar-liquid hygrometry (Forni *et al.*, 2018) and phase equilibria investigations (Fowler *et al.*, 2007; Cannatelli, 2012). Forni *et al.* (2018) used oxygen barometry to constrain the oxygen fugacity (f_{O_2}) for CI magmas to one log unit above the QFM buffer (QFM + 1), similar to results of phase equilibria studies of the CI (Bohron *et al.*, 2006; Fowler *et al.*, 2007), and Minopoli and Fondo Riccio eruptions (Cannatelli, 2012), where f_{O_2} between QFM and QFM + 1 best reproduces the composition and phase assemblage of natural samples.

Lithology of the crust underlying Campi Flegrei

Modelling AFC processes requires understanding potential lithologies magmas might encounter during crustal ascent beneath Campi Flegrei. Geophysical and heat flow constraints on the structure of the Campanian crust generally suggest a Moho depth of <25 km (Ferrucci *et al.*, 1989; Pontevivo & Panza, 2006; Nunziata, 2010). At $\lesssim 4$ km depth, borehole data indicate that the shallow crust is composed of buried pyroclastic sequences, intercalated with Upper Miocene sedimentary sequences (Rosi & Sbrana, 1987; D'Antonio, 2011; Piochi *et al.*, 2014). At $\gtrsim 4$ km, basement rocks are identified through their homogenous density in tomographic and gravity data (Battaglia *et al.*, 2008; Berrino *et al.*, 2008). However, due to similarities in their physical properties, the nature of the basement rocks beneath Campi Flegrei remains debated, with studies variously attributing it as Meso-Cenozoic carbonates (Judenherc & Zollo, 2004; Battaglia *et al.*, 2008; Zollo *et al.*, 2008), Palaeozoic metamorphic basement (previously termed Hercynian basement, e.g. Pappalardo *et al.*, 2002), or syenitic cumulate residue from past eruptions (Fowler *et al.*,

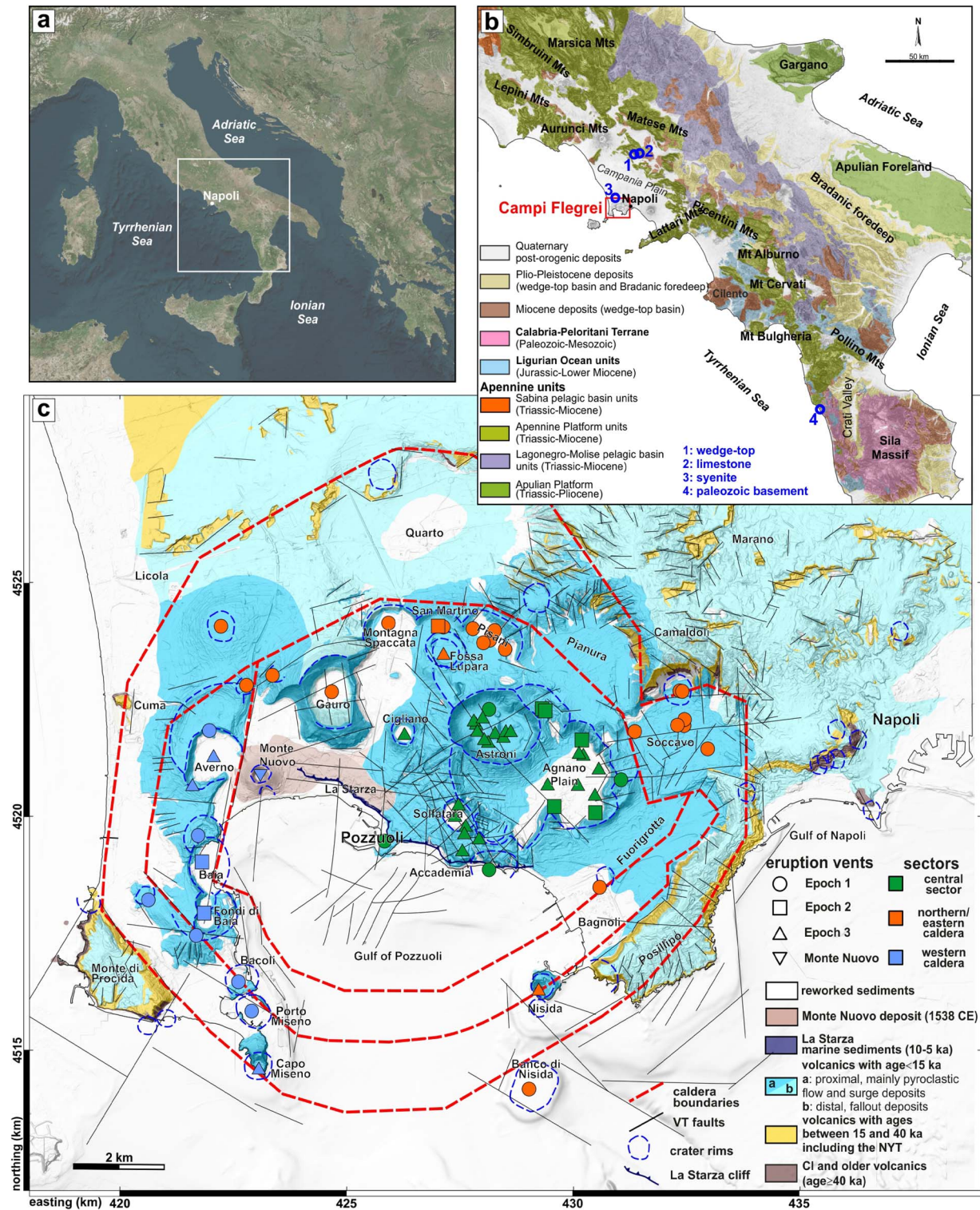


Fig. 1. Maps showing Campi Flegrei and vent locations of eruptions in the last 15 kyr. (a) Map of Italy showing the location of Campi Flegrei, square indicates area enlarged in (b) to show sampling locations of the basement rocks. (b) Simplified geological map of the southern Apennines showing distribution of tectonic units (Ciarcia & Vitale, 2025), and the locations the basement rocks were sampled: 1. Syn-orogenic wedge-top flysch, sample 23-FMR-003; 2. Limestone, sample 23-FMR-001; 3. Syenite, sample 23-FMR-014; 4. Palaeozoic gneiss, sample 23-FMR-017. (c) Simplified geological map of Campi Flegrei showing locations of the vents in the last 15 kyr, from Smith et al. (2011). Colours refer to the tectonic setting of the vents: orange are eruptions that occurred along the northern/eastern caldera rim faults; purple are eruptions with vents along regional and rim faults on the western side of the caldera; and in green are the eruptions from vents in the central eastern side of the caldera. Map also shows the distribution of pyroclastic deposits (Natale et al., 2024b, 2024a) and caldera and crater rims (Vitale & Isaia, 2014; Natale et al., 2022a). Vent ages refer to epochs defined in Smith et al. (2011).

2007; D'Antonio, 2011). Insights into the basement lithology are provided by erupted xenoliths, particularly the lithic-rich Breccia Museo unit of the CI (Fedele *et al.*, 2008), which contains plutonic syenite clasts (Fedele *et al.*, 2006; Gebauer *et al.*, 2014) in addition to hydrothermally altered lithic fragments from shallow lavas beneath the caldera (Di Vito *et al.*, 1999). Additionally, Pappalardo *et al.* (2002) identified two different xenolith types within deposits from the Minopoli 1 eruption; although the small clast size hampered detailed characterisation, these are suggested as deriving from Upper Miocene arenaceous sediments and the Palaeozoic metamorphic basement. Studies of isotopic variation in Campi Flegrei erupted products also provide information on potential crustal contamination sources: radiogenic and stable isotopic variation in magmas erupted in the last 60 kyr is attributed to interaction of the magmas with small amounts of both metamorphic Palaeozoic basement (~1–12% assimilation) and arenaceous sediments (<10% assimilation) Pappalardo *et al.*, 2002; D'Antonio *et al.*, 2007; Arienzo *et al.*, 2011; Di Renzo *et al.*, 2011; Iovine *et al.*, 2018). Despite the suggestion that assimilation plays a role in controlling the compositional evolution of Campi Flegrei magmas, this is yet to be empirically verified and the composition of the assimilant and extent of contamination are poorly defined.

ANALYTICAL METHODS

Sampling and sample preparation

To define the starting composition for our rhyolite-MELTS models, we analysed melt inclusions in samples of tephra from the three most mafic post-15 ka Campi Flegrei eruptions: Minopoli 1, Minopoli 2 and Fondo Riccio (Smith *et al.*, 2011). Samples CF9 (Minopoli 2) and CF13 (Minopoli 1) were sampled by Smith *et al.* (2011) and sample CF410 (Fondo Riccio) was collected during fieldwork for this project in March 2022 (UTM 423047E, 4523062 N). Samples were crushed and sieved, with clinopyroxene phenocrysts handpicked from the 250–500 μm size fraction.

Potential basement lithologies that might have contaminated Campi Flegrei magmas were sampled during fieldwork in May 2023. Sampling locations are given in Fig. 1b and the Supplementary Material Table S1. These include an upper Jurassic–lower Cretaceous limestone (sample 23-FMR-001, unit Gcb of Vitale & Ciarcia, 2018, no. 2 in Fig. 1b); Upper Miocene syn-orogenic wedge-top deposits (previously termed flysch, Fowler *et al.*, 2007; sample 23-FMR-003, unit CVTg of Vitale & Ciarcia, 2018, no. 1 in Fig. 1b); Palaeozoic gneiss (sample 23-FMR-017, Sila unit of Graessner & Schenk, 2001; Filice *et al.*, 2015, no. 4 in Fig. 1b); and a syenitic xenolith from the Breccia Museo (sample 23-FMR-014, no. 3 in Fig. 1b). These whole rocks were crushed in a tungsten carbide jaw crusher before being ground in an agate TEMA mill.

Electron probe microanalysis

Clinopyroxene phenocrysts from mafic Campi Flegrei eruptions were picked from tephra samples, mounted in epoxy, ground and polished for analysis. Crystals and melt inclusions were analysed using a JEOL JXA 8200 wavelength-dispersive electron microprobe in the Research Laboratory for Archaeology and the History of Art, University of Oxford, UK. All analyses were conducted with a 15kV accelerating voltage and a 6nA beam current and 10 μm beam diameter were used to analyse the melt inclusions, while a 25 nA current and 3 μm beam were used to analyse the host crystals. Appropriate natural and synthetic standards were used for calibration, and the MPI-DING reference glasses (Jochum *et al.*, 2006) were analysed as secondary standards to

check the accuracy and reproducibility of results, compared to the preferred values. Accuracy was typically better than 2% with precision typically $\pm 0.5\%$ RSD for Si and $\sim \pm 3\%$ for most other major elements except for Na ($\sim \pm 11\%$) and low abundance elements Ti ($\pm 6\%$) and Mn ($\pm 16\%$). All Fe is assumed to occur as FeO (FeO(t)). All electron probe microanalysis (EPMA) analyses are included in Table S2; from this survey of melt inclusions and their host crystals, we selected the starting composition for our rhyolite-MELTS models.

X-ray fluorescence analysis

The crustal samples were prepared as fused glass beads and pressed powder pellets for whole-rock major (>1 wt %) and trace (<1 wt %) element analysis, respectively. Analyses were performed using the Zetium wavelength dispersive (WD) X-ray fluorescence (XRF) in the Earth Surface Research Lab, Trinity College Dublin, following the methods described in Carter *et al.* (2024). From measurements of secondary standards analysed alongside the samples, accuracy is <2% for major and 5–10% for trace elements, and precision (in terms of relative standard deviation, standard deviation/mean) is generally <1% for major elements and <2% for trace elements. Data are included in Table S1.

LITERATURE DATA

Matrix glass data from post-15 ka Campi Flegrei eruptions were compiled from the literature for comparison with rhyolite-MELTS outputs (Table S3). While bulk-rock and melt inclusion analyses might record liquid compositions, these can be affected by crystal accumulation/fractionation (Passmore *et al.*, 2012; Higgins & Stock, 2024) and post-entrapment processes (Lowenstern, 1995; Cannatelli *et al.*, 2016) and we exclude them from our analyses, instead preferring to limit the risk of misinterpretation by like-for-like directly comparing the last liquid remaining in the magmatic system before eruption. We investigate the processes affecting major element variability between eruptions, which does not preclude other processes, such as volatile fluxing and magma mixing, that have been reported for post-15 ka erupted products (Di Renzo *et al.*, 2011; Arienzo *et al.*, 2016). The compositions of natural glasses erupted from Campi Flegrei in the past 15 kyr were compiled from the GEOROC database (Sarbas, 2008); this yielded glass analyses from 48 eruptions and ~ 1900 analyses in total (Di Girolamo *et al.*, 1984; de Vita *et al.*, 1999; Brocchini *et al.*, 2001; Romano *et al.*, 2003; Piochi *et al.*, 2008; Smith *et al.*, 2011; Fourmentraux *et al.*, 2012; Tomlinson *et al.*, 2012; Arienzo *et al.*, 2016; Stock *et al.*, 2018). Of these, 1036 matrix glass analyses are from 6 western caldera eruptions, 620 are from 20 northern/eastern caldera eruptions and 255 are from 22 central caldera eruptions. No glass data are currently available for other post-15 ka eruptions (~ 20 eruptions in total; Smith *et al.*, 2011). There was no systematic difference in glass compositions between studies. Due to the number of glass compositions in our dataset, the uncertainty of the EPMA measurements collapse in, assuming a normal distribution. Therefore, any misfit between models and the data are probably not an artefact of EPMA uncertainty.

RHYOLITE-MELTS THERMODYNAMIC MODELLING

We modelled the stable phase assemblages and major element compositional evolution of the liquid phase in Campi Flegrei during FC and AFC using the rhyolite-MELTS thermodynamic

modelling software, which calculates the stable phase assemblage in a system under a given set of conditions based on minimisation of free energy, with the thermodynamic properties of each phase calibrated from experiments (Gualda *et al.*, 2012). We used rhyolite-MELTS v.1.2., which has a coupled H₂O–CO₂ fluid saturation model and the most comprehensive calibration dataset to date (Ghiorso & Gualda, 2015). The models were run using the alphaMELTS2 front-end (Smith & Asimow, 2005), with a Python-based script designed to batch run simulations over a range of potential storage conditions (see Gainsforth *et al.*, 2015; Antoshechkina & Ghiorso, 2018; Gleeson *et al.*, 2023). We model fractional crystallisation as opposed to equilibrium crystallisation, following previous thermodynamic modelling (Fowler *et al.*, 2007; Cannatelli, 2012) and empirical major element geochemical studies (Civetta *et al.*, 1991), which suggest that this process best describes the relationship between the compositions of Campi Flegrei erupted products.

Despite previous studies identifying isotopic heterogeneity in Campi Flegrei erupted compositions (D'Antonio *et al.*, 2007; Arienzo *et al.*, 2010; Di Renzo *et al.*, 2011) and suggesting separate end-member magma batches, these are not reflected in variations in major element chemistry, where eruptions can be related by crystallisation to a single parental magma (Civetta *et al.*, 1991; Smith *et al.*, 2011). We therefore model crystallisation of a single parental magma, using the most primitive melt inclusion that we measured in mafic post-15 ka eruptions as the starting composition in our models (CF410_cpx12_MI18; Table S2). This clinopyroxene-hosted inclusion from Fondo Riccio has the highest MgO (6.23 wt %) and CaO (11.62 wt %) concentrations in our dataset and low incompatible element concentrations (Na₂O+K₂O 6.84 wt %), and is in equilibrium with its host crystal based on their $K_D(\text{Fe-Mg})^{\text{cpx-liq}}$ of 0.31 ± 0.07 (i.e. within the equilibrium range of 0.28 ± 0.08 from Putirka (2008). Masotta *et al.* (2013) identified that melt alkali content can affect these calculations, but their revised model converges with the $K_D(\text{Fe-Mg})^{\text{cpx-liq}}$ range given in Putirka (2008) for $K_D > 0.2$, so we prefer to use this as it does not require prior knowledge of crystallisation temperature, although the narrow range likely reflects the majority of published experiments involving mafic systems with the actual equilibrium range potentially being larger (Di Fiore *et al.*, 2021). The selected melt inclusion is glassy, implying post-entrapment crystallisation (PEC) has not been extensive (Fig. S1) and a correction for PEC did not significantly alter our model outputs (Fig. S2). Although previous authors have reported more mafic melt inclusions (Webster *et al.*, 2003; Cannatelli *et al.*, 2007), they require extensive correction for post-entrapment crystallisation, which can compromise their major element composition (Danyushevsky *et al.*, 2002; Kress & Ghiorso, 2004), so we prefer to use our own direct measurements.

Fractional crystallisation models

We initiated our FC models at the calculated liquidus and ended at a melt fraction of ~0.05 (5%; models fail closer to the solidus, likely due to extreme incompatible element enrichment in the melt phase), with a temperature step of 1 °C. The proportions and compositions of all stable phases are recorded at each temperature step, with crystals removed from the bulk composition between steps. No constraints were placed on the phases rhyolite-MELTS could stabilise; predicted phases were compared to those observed in natural samples. Model parameters (L_{fO_2} , P , L_{H_2O}) are defined for each model and, to constrain the conditions of Campi Flegrei magma storage, we varied these parameters across the range of possible conditions previously identified in the

literature (Table 1). We varied L_{fO_2} by fixing it above the liquidus and then allowing fO_2 to vary unbuffered below the liquidus. In our FC models, we tested a matrix of parameter space so that each intensive variable was tested against the full range of the remaining two, totalling 1720 individual simulations. To reduce the modelled parameter space, we follow previous studies in only considering isobaric crystallisation (Fowler *et al.*, 2007; Cannatelli, 2012; Rooney *et al.*, 2012; Stock *et al.*, 2016; Gleeson *et al.*, 2017). While previous authors have suggested that the Campi Flegrei sub-volcanic system could have magmas stored at multiple depths (Astbury *et al.*, 2018; Giordano & Caricchi, 2022), we find the liquid lines of descent produced in our rhyolite-MELTS models are not sensitive to polybaric crystallisation in the mid- to upper-crust within a reasonable pressure range (Fig. S3) and so consider only a simple isobaric scenario.

Assimilation models

Following Fowler *et al.* (2007), we model AFC taking the best-fit intensive parameters for each volcano-tectonic setting based on the results obtained from FC simulations (see section Statistical determination of best-fit storage conditions, below) before adding a contaminant to rhyolite-MELTS models at a fixed temperature, using the bulk compositions measured from samples of the basement lithology (Table S1; sample 23-FMR-001 = limestone; sample 23-FMR-003 = wedge-top deposits; sample 23-FMR-14A = syenite; sample 23-FMR-017 = Palaeozoic metamorphic basement). In each AFC model, we systematically varied the type and amount of assimilation, holding all other model parameters constant and producing 80 additional models. While we acknowledge that this is a simplification, simultaneously changing the type of assimilant, temperature interval over which contamination occurs, conditions of magma storage (P , L_{fO_2} , L_{H_2O}) and adding mixtures of different assimilants creates an unmanageably large parameter space. Instead, our approach assumes that the intrinsic conditions of magma storage exert a first-order control on the liquid line of descent and that small amounts of assimilation of a dominant assimilant composition have a second-order impact. Rhyolite-MELTS can simulate assimilation under either isenthalpic or isothermal conditions (Ghiorso & Kelemen, 1987), which can constrain different aspects of assimilation. To investigate the effect of different assimilant compositions on the liquid line of descent in a long-lived magmatic system, we follow Fowler *et al.* (2007) in running AFC models isothermally, whereby the initial temperature of the assimilant is the same as the melt. Each model was run as a closed system FC simulation from the liquidus to 1100 °C before the assimilant was added and chemically equilibrated with the new system. The melt then evolved once again down to low melt fractions, reducing temperature by 1 °C and extracting crystals at each step, as in FC models. The amount of assimilant was varied between $M_a/M_m = 0.01$ –0.3 in 0.05 increments, where M_a/M_m is the ratio of assimilant to melt (equivalent to 1–30% contamination).

Statistical determination of best-fit storage conditions

Most previous studies that have determined magmatic processes/storage conditions by correlating the compositions of natural erupted materials with rhyolite-MELTS outputs have qualitatively identified the best-fit model run conditions 'by eye' (Fowler *et al.*, 2007; Fowler & Spera, 2010; Cannatelli, 2012). This approach was advanced by Gleeson *et al.* (2017), who employed a statistical method based on least-squares analysis to quantitatively determine the best-fit model conditions, comparing the residuals between

Table 1: Magma storage conditions investigated in rhyolite-MELTS models and the ranges over which they were varied

Intensive parameter	Range tested	Intervals	References
Pressure (MPa)	50 to 500	50	Bohrson <i>et al.</i> , 2006; Cannatelli <i>et al.</i> , 2007; Fowler <i>et al.</i> , 2007; Zollo <i>et al.</i> , 2008; Arienzo <i>et al.</i> , 2016
Initial water content (wt %)	0.5, 1 to 6	1	Mangiacapra <i>et al.</i> , 2008; Arienzo <i>et al.</i> , 2016; Stock <i>et al.</i> , 2016; Forni <i>et al.</i> , 2018
Oxygen fugacity (log units relative to the quartz–fayalite–magnetite buffer)	–2 to +3	1	Fowler <i>et al.</i> , 2007; Cannatelli, 2012; Stock <i>et al.</i> , 2016

The ranges chosen were constrained based on previous studies of Campi Flegrei.

compositional evolution of the modelled melt phase and whole-rock samples from Aluto volcano (Ethiopia). We build on this work, implementing an improved statistical assessment to determine the correlation between each of our 1800 (1720 FC and 80 AFC) rhyolite-MELTS models and natural matrix glasses from Campi Flegrei. Rather than comparing models against our full literature dataset, we separate post-15 ka Campi Flegrei glasses into three groups, based on the volcano-tectonic setting of their eruption vents (i.e. western caldera eruptions, northern/eastern caldera eruptions, central caldera eruptions) to identify changes in magma storage conditions and/or processes across the caldera.

Our statistical procedure for identifying best-fit models is as follows: for each oxide output by rhyolite-MELTS (except P_2O_5 which is in too low concentration), we calculated the root mean square error (RMSE) between the modelled liquid line of descent and natural Campi Flegrei matrix glasses following Willmott (1981):

$$RMSE_A = \sqrt{\frac{\sum_i^n (y_{i,A} - \hat{y}_{i,A})^2}{n}} \quad (1)$$

where $RMSE_A$ is the root mean square error for oxide A, n is the number of natural samples whose composition we are comparing against rhyolite-MELTS outputs; $y_{i,A}$ is the concentration of major oxide A in natural sample i at a given MgO concentration and $\hat{y}_{i,A}$ is the concentration major oxide A predicted by rhyolite-MELTS for the same MgO concentration. In this approach, MgO is an index of fractionation, decreasing along the liquid line of descent as it is incorporated into phases such as olivine, clinopyroxene and spinel group minerals.

The RMSE is in units of the variable y (in our case, wt %) and, as the concentration of major oxides varies considerably in natural volcanic glasses (e.g. ~1 wt % TiO_2 to >50% SiO_2 in our samples), the magnitude of RMSE varies accordingly. As a result, we normalised each RMSE value to the average concentration of the major oxide in our natural Campi Flegrei matrix glasses:

$$RMSE_{norm,A} = \frac{RMSE_A}{\bar{X}_A} \quad (2)$$

where $RMSE_{norm,A}$ is the normalised root mean square error for oxide A and \bar{X}_A is mean concentration of oxide A in all of our natural Campi Flegrei glasses.

The $RMSE_{norm}$ values for each major oxide were then summed to give a single, total RMSE ($RMSE_{total}$) for each model:

$$RMSE_{total} = \sum RMSE_{norm} \quad (3)$$

By identifying our rhyolite-MELTS model that produces the lowest $RMSE_{total}$, we constrained the input conditions that best

reproduce the liquid line of descent recorded by natural Campi Flegrei erupted products and thus mirror the most likely conditions of sub-volcanic magma storage. We have provided a sample Python code to calculate the RMSE of rhyolite-MELTS models at [doi:10.5281/zenodo.14900107](https://doi.org/10.5281/zenodo.14900107). Our approach builds on the work of Gleeson *et al.* (2017) by comparing rhyolite-MELTS outputs to natural data throughout the entire crystallisation sequence from the most mafic to evolved samples, assessing which combination of intensive parameters best reproduces the observed liquid line of descent.

Our statistical measure of the best-fit conditions was supplemented by comparison of the phase assemblages predicted by rhyolite-MELTS and those observed in natural samples (see Fractional crystallisation models, below).

Potential limitations of rhyolite-MELTS

Previous studies using MELTS to constrain magma storage conditions, including those for the petrogenesis of the CI, note a displacement of up to ~3 wt % between predicted melt K_2O and CaO concentrations and those measured in natural samples (Fowler *et al.*, 2007; Fowler & Spera, 2010). The CaO discrepancy is likely due to under-stabilisation of clinopyroxene (Fowler & Spera, 2010), whereas the K_2O discrepancy may be the result of MELTS over stabilising sanidine due to a paucity of experimental data available for calibrating the alkali feldspar–liquid equilibria (Gualda *et al.*, 2012). The calibration of rhyolite-MELTS used in this study (v1.2.) remedies this issue by adjusting the stability of quartz and the potassium end-member of alkali feldspar and hence is more suitable for the alkali Campi Flegrei magmas (Gualda *et al.*, 2012). Rooney *et al.* (2012) note that rhyolite-MELTS also overpredicts melt P_2O_5 concentrations, which they attribute to inaccuracies in the apatite solubility model. However, due to the low P_2O_5 concentrations in all our natural Campi Flegrei samples (generally approaching the lower limit of detection), this element is not considered in our subsequent estimates of best-fit storage conditions.

Rhyolite-MELTS is inherently limited by a lack of hydrous phase-bearing experiments and thermodynamic models for hydrous mafic silicates, making it largely inappropriate for systems where hydrous minerals are major phases controlling the liquid line of descent (e.g. amphibole-rich rhyolites; Gualda *et al.*, 2012). However, in Campi Flegrei hydrous minerals (e.g. biotite, apatite) are ubiquitously minor phases (Isaia *et al.*, 2004; Smith *et al.*, 2011; Stock *et al.*, 2018); hence, we expect inaccuracies in reproducing hydrous mineral stabilities will have minimal impact on our model outputs. Sanidine compositions calculated by rhyolite-MELTS are also more sodic than observed in natural samples, with sanidine appearing on the liquidus at higher temperatures (~40 °C) compared to thermometry and experiments on natural systems (Gualda *et al.*, 2012; Gardner *et al.*, 2014; Gleeson *et al.*, 2017). However, as sanidine generally appears at low melt fractions (Fowler *et al.*, 2007; Cannatelli, 2012),

it is also unlikely to significantly impact our model results for the questions posed in this study.

Rhyolite-MELTS remains an extremely valuable tool for evaluating how reasonable different scenarios are (FC and AFC), despite model inaccuracies largely related to the availability of experimental data. It has been successfully applied to model phase equilibria across a range of volcanic systems (e.g. recently [Knafele et al., 2020](#); [Boschetti et al., 2022](#); [Fred et al., 2022](#)). By comparing the fit of models run over a wide range of starting conditions to the natural data from Campi Flegrei, we can place new constraints on processes operating in the sub-volcanic system.

RESULTS

Compositional variation in post-15 ka Campi Flegrei glasses

Post-15 ka Campi Flegrei eruptions derived from vents in the three volcano-tectonic groups have distinct matrix glass compositions (although some overlap between compositions exists, [Fig. 2](#), [D'Antonio et al., 1999](#); [Di Renzo et al., 2011](#); [Smith et al., 2011](#)). The northern and eastern caldera eruptions are the most mafic (typically shoshonite–tephriphonolite) with the highest MgO, FeO and CaO concentrations and the lowest SiO₂ content. The Minopoli 2 eruption forms a distinct high MgO group separate from other eruptions ([Fig. 2](#)). The western caldera eruptions extend to the most evolved compositions (trachyte–phonolite), with low MgO, high SiO₂ and elevated Na₂O concentrations, forming a distinct low-K₂O, high-SiO₂ group ([Fig. 2c](#)). At very low MgO concentrations, the western caldera eruptions also tend towards elevated TiO₂ and Na₂O and depleted K₂O. The central caldera eruptions are typically intermediate between the other two groups in terms of their extent of evolution, ranging from tephriphonolites to phonolites/trachytes. They have the highest K₂O concentrations and variable Al₂O₃.

Fractional crystallisation models

All our FC models show comparable geochemical trends with phases coming onto the liquidus in a similar order ([Fig. 3](#)). Depending on the intensive parameters, olivine or clinopyroxene are the liquidus phases (1100–1180 °C) for all models, with clinopyroxene being the second phase to precipitate if not on the liquidus ([Fig. S4](#)). Spinel group minerals (predominantly magnetite; typically 1050–1120 °C) and plagioclase (typically 975–1050 °C) precipitate next but their saturation temperatures depend strongly on the model pressure, L_{H2O} and L_{fO2} (see below). Small amounts of biotite (890–945 °C), K-feldspar (sanidine; 805–890 °C) and, in some models, leucite (800–950 °C) come onto the liquidus at low temperatures. In a small number of models, olivine (~850 °C), nepheline (720–735 °C), garnet (705 °C) or muscovite (~730 °C) precipitate close to the solidus. Aside from these occasional near-solidus phases, the modelled phase assemblage mirrors that observed in post-15 ka Campi Flegrei eruptions ([Stock et al., 2018](#)).

Regarding the liquid line of descent, clinopyroxene-only crystallisation drives a decrease in MgO and CaO (from ~6 to 4.5 wt % and 11 to 9.5 wt % at *spinel-in*, respectively), with other oxides (Al₂O₃, K₂O, Na₂O, FeO, TiO₂) increasing in the residual liquid at high melt fractions, with FeO and TiO₂ beginning to decrease when spinel group minerals come onto the liquidus and the liquid evolves from shoshonite to latite. The onset of plagioclase crystallisation causes an inflection in Al₂O₃ with decreasing MgO as crystallisation continues, where Al₂O₃ becomes compatible in the crystallising assemblage and the liquid evolves from latite

to tephriphonolite; plagioclase is initially Ca-rich, further driving the decrease in the liquid CaO concentration, but becomes increasingly sodic at lower temperatures, reducing the rate of Na₂O enrichment in the liquid. K-feldspar comes onto the liquidus when MgO has decreased to ~0.2 wt %; at this point K₂O becomes compatible in the crystallising assemblage and is depleted in the residual liquid, with the liquid evolving towards phonolite. This is accompanied by a sharp Na₂O enrichment in the liquid as the fraction of crystallising plagioclase decreases. Sharp compositional changes at very low MgO contents in both FC and AFC models ([Fig. 4e](#)) are likely a result of limitations modelling minor minerals, which accommodate incompatible elements at low melt fractions ([Gualda et al., 2012](#)). Although these trends hold generally for each of our simulations, the exact nature of the liquid line of descent depends on the liquidus temperature of each mineral phase and the proportions of crystallising solid, which vary as a function of the model intensive parameters.

Varying the initial H₂O content

Although varying L_{H2O} does not have a significant effect on the type or order of minerals crystallising in our rhyolite-MELTS models ([Fig. S5](#)), small differences in their solidus temperatures, modal proportions and compositions have significant effects on the liquid line of descent ([Fig. 4](#)). This is particularly the case for plagioclase, where crystal anorthite contents are highly sensitive to the H₂O content of their equilibrium melt ([Lange et al., 2009](#)). At low L_{H2O} (~0.5–3 wt %), feldspar minerals stop crystallising at relatively high temperatures (~775–850 °C), leading K₂O to behave incompatibly in the crystallising assemblage at low temperatures (below 800 °C) and MgO contents. Conversely, at high L_{H2O} (~4–6 wt %), feldspar continues to crystallise until the solidus and CaO behaves incompatibly in the melt at low temperatures (below ~810 °C). Reducing L_{H2O} to <4% significantly reduces sanidine stability, resulting in very high melt Al₂O₃ contents (20–22 wt %; [Fig. 4a](#)). Prediction of sanidine compositions is a known limitation of rhyolite-MELTS ([Gualda et al., 2012](#); [Gardner et al., 2014](#)), which might explain these differences. Higher L_{H2O} leads to a greater proportion of feldspar crystallising overall (~0.47 for 6 wt % L_{H2O} compared to ~0.38 for 1 wt %, largely due to differences in the amount of sanidine predicted to crystallise). Initial melt H₂O content also has an impact on the predicted clinopyroxene composition, which affects the melt TiO₂ content. At high L_{H2O} (>3%), clinopyroxene has higher TiO₂ contents, especially at high temperatures, so crystallisation strongly drives down the melt TiO₂ content, whereas at lower L_{H2O} (<2%), clinopyroxene TiO₂ content is much lower until low temperatures, so the TiO₂ content remains elevated ([Fig. 4c](#)). Increasing L_{H2O} reduces the TiO₂ content of spinel group minerals, but the small quantities (~0.05) of spinel group minerals crystallised means the effect on melt TiO₂ content is minimal compared to clinopyroxene.

Varying oxygen fugacity

Increasing L_{fO2} in our rhyolite-MELTS models increases the stability of spinel group minerals, which primarily impacts the SiO₂ and FeO concentrations of the residual melt during fractional crystallisation: under more oxidising conditions, where spinel group minerals stabilise at higher temperatures, melt SiO₂ concentrations begin to increase at higher temperatures and FeO contents are lower for any given MgO content ([Fig. 4e](#)). The earlier precipitation of spinel group minerals under more oxidising conditions is consistent with experimental studies ([Toplis & Carroll, 1995](#); [Feig et al., 2010](#)). Varying L_{fO2} also effects the liquid line of descent for TiO₂ with generally lower melt TiO₂ concentrations

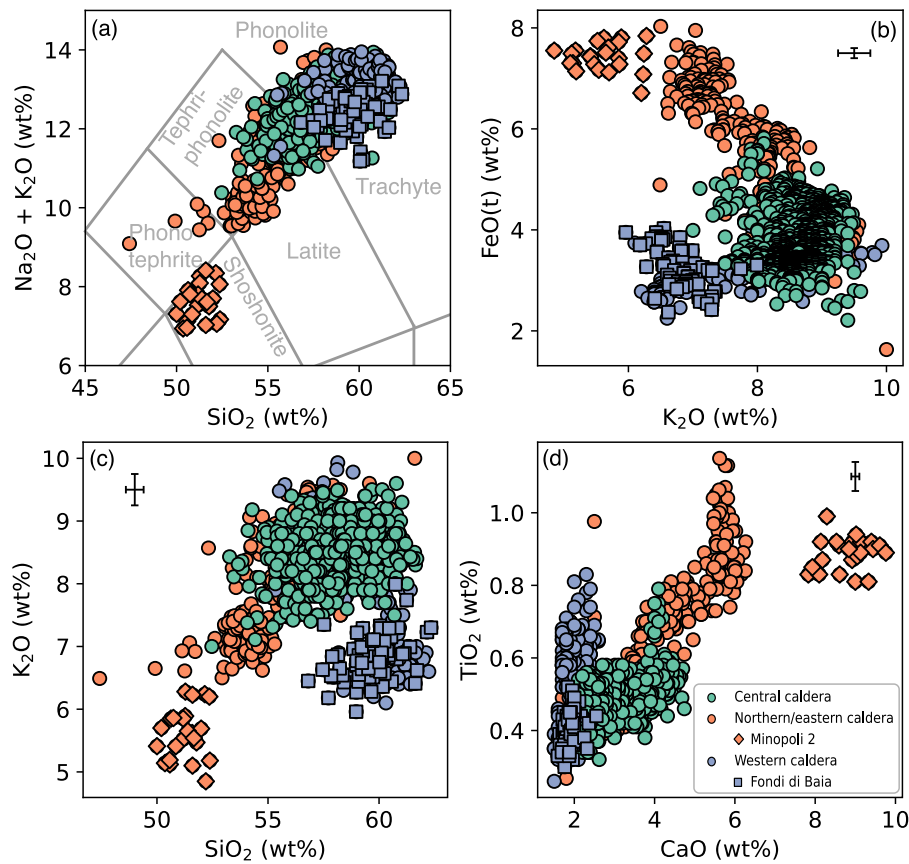


Fig. 2. Major element variation diagrams of literature glass data for Campi Flegrei eruptions in the last 15 kyr. Points are coloured by tectonic group as illustrated in Fig. 1. Error bars show representative 2 SD error from EPMA analysis from Smith et al. (2011). Glass data were compiled from GEOROC, see Literature data for references. Glass data from Minopoli 2 eruption, which forms a distinct high-MgO group, are shown with diamond markers and data from the Fondi di Baia eruption, which is discussed in the Assimilation at Fondi di Baia section, are shown with square markers.

in the more oxidised models, again because of the earlier spinel group minerals fractionation but also differences in the predicted clinopyroxene composition, which initially contains more TiO_2 (Fig. 4f). However, at QFM+3, spinel minerals contain less TiO_2 than at QFM, so at lower $L_{f\text{O}_2}$, there is a steeper reduction of TiO_2 in the melt after spinel-in.

Varying pressure

Changing pressure in our rhyolite-MELTS models has minor impacts on the predicted phase assemblage. The major mineral phases observed in Campi Flegrei erupted products—clinopyroxene, plagioclase feldspar, alkali feldspar—are predicted to crystallise across all pressures (Figs 3 and S4). However, at high pressures (>200 MPa), rhyolite-MELTS predicts minor muscovite and garnet crystallisation close to the solidus (Fig. 3c). Likewise, at low pressures (<70 MPa), leucite is predicted to crystallise in significant quantities (~7%, Fig. 3a). The liquid line of descent is not very sensitive to pressure; for all major oxides there is generally <1 wt % difference in the predicted concentration of the oxide at equivalent MgO/temperature steps across the entire range of pressures (Fig. 4g–i). Small differences between models run at opposing ends of our pressure range observed at low temperature likely reflect the crystallisation of near-solidus muscovite, garnet and leucite.

Modelling assimilation—fractional crystallisation

The major and trace element compositions of basement rocks, which represent potential Campi Flegrei assimilants are listed in

Table S1. The addition of an assimilant to our rhyolite-MELTS models produces similar geochemical trends for all volcanotectonic groups, although these trends differ for each assimilant composition.

Assimilation of Palaeozoic metamorphic basement

The addition of Palaeozoic metamorphic basement assimilant to our rhyolite-MELTS models significantly increases the predicted melt SiO_2 content and reduces the predicted Al_2O_3 content, relative to FC models run with the same set of intensive variables (Figs S8, S12 and S16); these effects increase with increasing quantities of the contaminant. Small quantities of Palaeozoic metamorphic contamination cause melt K_2O and Na_2O contents to increase at low temperatures and melt fractions, due to changes in the predicted phase assemblage: in models with $M_a/M_m = 0.1$ feldspar stops crystallising ~80 °C higher temperature than for $M_a/M_m = 0.3$. For models with $M_a/M_m > 0.2$, rhyolite-MELTS predicts crystallisation of quartz at low temperatures.

Assimilation of syn-orogenic wedge-top deposits

Addition of wedge-top deposits increases the predicted SiO_2 content of the melt in our rhyolite-MELTS models compared to FC under equivalent storage conditions, especially at low temperatures and melt fractions (Figs S7, S11 and S15); at $M_a/M_m = 0.3$, the SiO_2 content of the residual melt is predicted to reach ~72 wt % at low temperatures. Addition of wedge-top deposits also slightly increases the predicted melt CaO concentration and decreases the melt FeO, K_2O , Na_2O and Al_2O_3 at equivalent MgO content

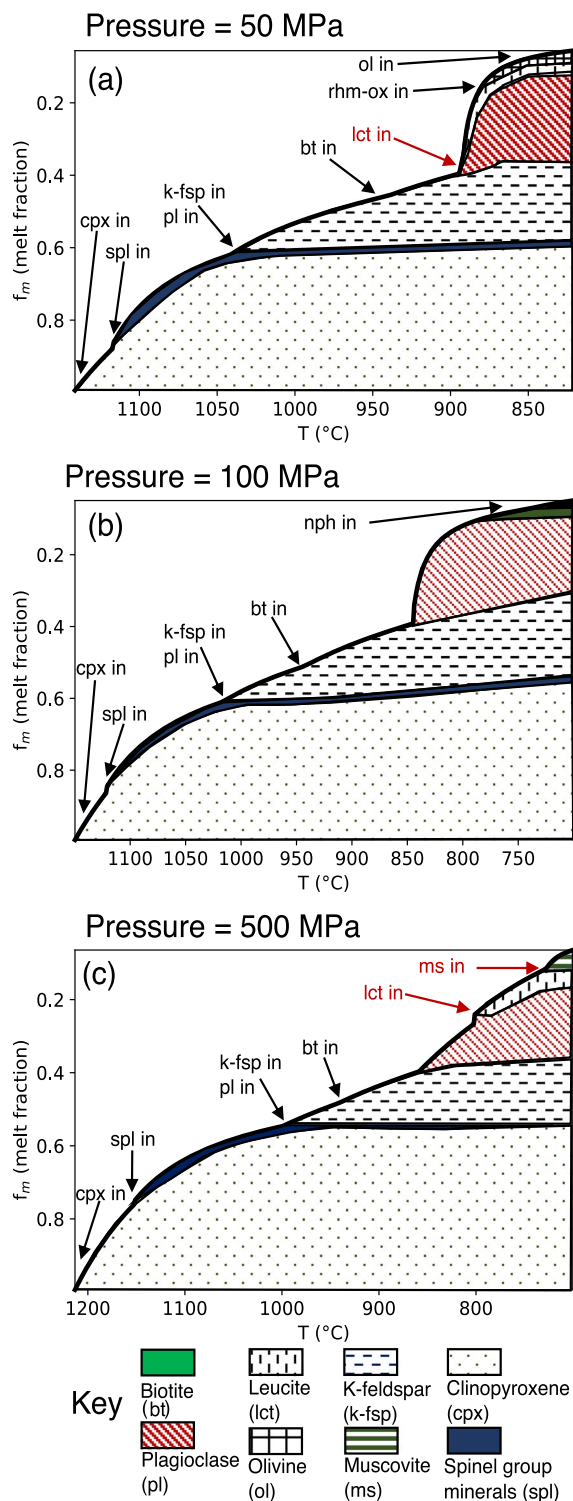


Fig. 3. Phase proportions as a function of magma temperature for fractional crystallisation MELTS models at different pressures. Models are run at $L_{fO_2} = \text{QFM} + 1$ and $L_{H_2O} = 2$ wt %. Phases highlighted in red (leucite, muscovite) are not observed in natural Campi Flegrei samples in the major crystallising assemblage. Phases not in key: nph, nepheline; rhm-ox, rhombohedral oxide

compared to FC models with the same intensive parameters, with the magnitude of these changes increasing with the amount of assimilate. For small amounts of wedge-top deposit assimilation, sanidine stops crystallising at higher temperatures, leading

to K_2O incompatibility at low temperatures, whereas larger amounts of wedge-top deposit assimilation causes more Na-rich plagioclase to crystallise, lowering the Na_2O contents of the residual melt.

Assimilation of limestone

Addition of limestone in our rhyolite-MELTS models has the most significant impact on the predicted CaO concentration (Figs S6, S10 and S14), causing it to increase relative to FC models run with the same intensive parameters. Conversely, the predicted liquid SiO_2 content is much lower relative to equivalent FC models at a given MgO concentration. These effects increase with greater amounts of limestone contamination, especially at $M_a/M_m > 0.01$ (Figs S6, S10 and S14). To a lesser extent, at equivalent melt MgO content, limestone assimilation causes slightly lower FeO and Al_2O_3 contents and slightly higher TiO_2 relative to equivalent FC models and with limestone addition at $M_a/M_m > 0.05$ rhyolite-MELTS predicts minor garnet crystallisation at best-fitting intensive parameters for uncontaminated FC.

Assimilation of syenite

Where a syenite assimilate is added to our rhyolite-MELTS models, melt SiO_2 contents are higher and Al_2O_3 contents are lower than in FC models run under equivalent conditions at the same melt MgO content, due to greater proportions of crystallising feldspar. For the other major oxides, adding syenite does not significantly change the liquid line of descent compared to equivalent FC models, saving a small reduction in K_2O content and increase in Na_2O , CaO and TiO_2 concentrations. In all cases, the predicted liquid lines of descent are similar irrespective of the quantity of contaminant (Figs S9, S13 and S17).

DISCUSSION

Constraints on magma storage conditions

Contrasting major element compositions of matrix glasses erupted from vents in different volcano-tectonic settings allude to variations in the structure and/or processes operating within the sub-volcanic plumbing system in different parts of the Campi Flegrei caldera. Changing L_{H_2O} , L_{fO_2} and P in our models affects the predicted liquid line of descent (Fig. 4), which in turn controls how well the models match measured natural glass compositions from Campi Flegrei (Fig. 5). Our RMSE statistical test constrains the combination of intensive parameters, which produce the best-fit between the liquid line of descent predicted by rhyolite-MELTS FC models and that recorded by natural glass compositions (Table 2 and S4–S6).

Liquidus H_2O concentration

Varying L_{H_2O} between 1 and 6 wt % markedly changes the stability of feldspar, with *feldspar-in* occurring at higher temperatures for lower H_2O contents, as observed in previous experimental (Eggler, 1972; Gaetani et al., 1993; Sisson & Grove, 1993; Lange et al., 2009), MELTS based studies (Fowler et al., 2007; Cannatelli, 2012) and observations of erupted plagioclase textures and compositions (e.g. at Stromboli—Landi et al., 2004). At the lower end of our L_{H_2O} range (0.5–2 wt %), our models predict an enrichment in the melt K_2O at low temperatures (i.e. incompatible behaviour) and consistently high melt TiO_2 contents, which are not observed in natural Campi Flegrei samples (Fig. 6). Similarly, at the top of our L_{H_2O} range (5–6 wt %), rhyolite-MELTS predicts that the melt becomes enriched in CaO at low temperatures, with consistently low TiO_2 and high Al_2O_3 concentrations, which are also not

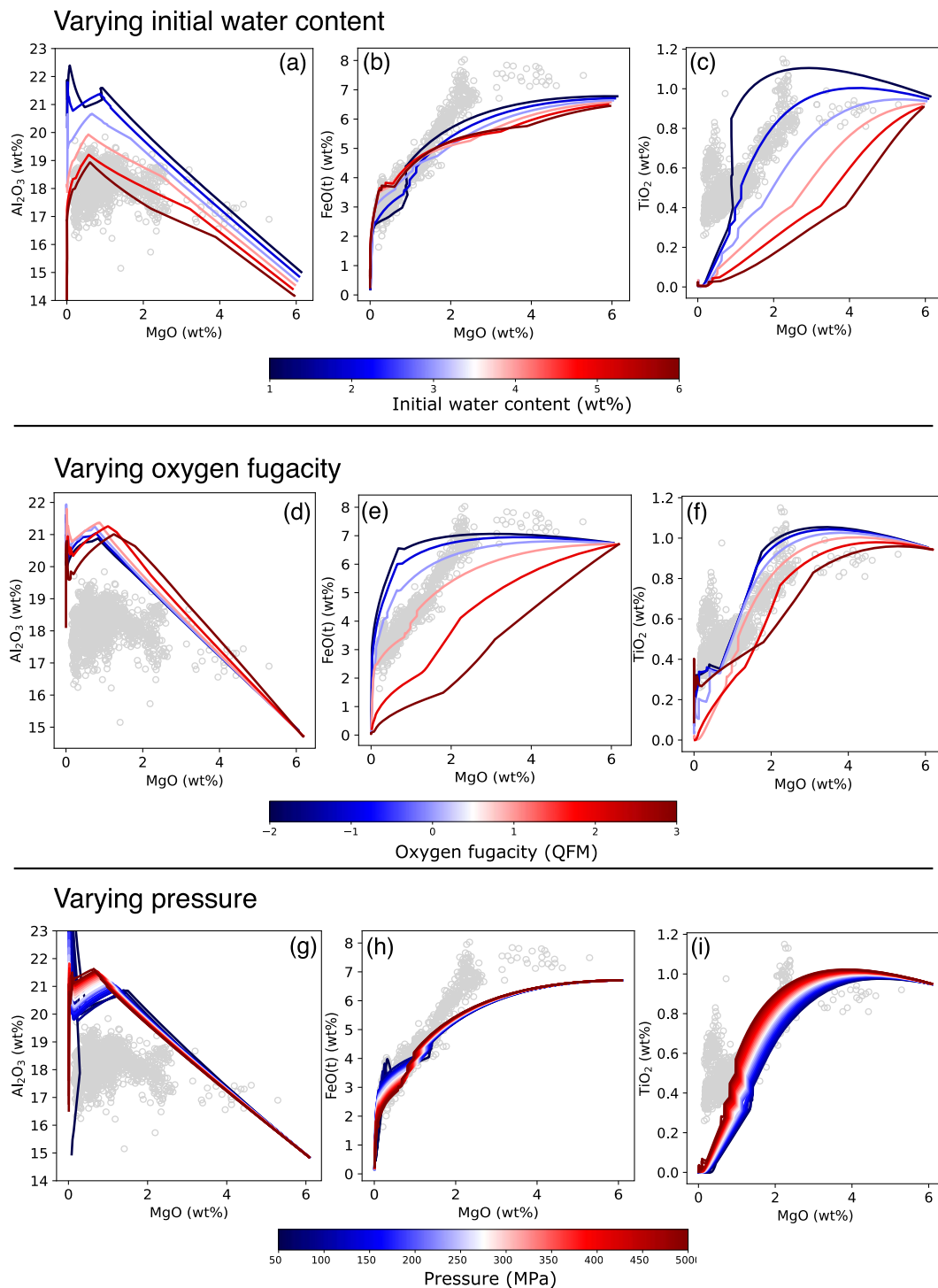


Fig. 4. The effect of varying each intensive parameter on the resulting liquid line of descent predicted by rhyolite-MELTS. The colour of the line represents the value of the intensive parameter being varied (where blue to red indicates the intensive parameter increasing from the lowest to highest value tested): $L_{\text{H}_2\text{O}}$ from 1–6 wt % in (a), (b), (c); L_{fO_2} from –2 to +3 log units below/above the QFM buffer in (d), (e), (f); pressure from 50 to 500 MPa in (g), (h), (i). For (a)–(f), pressure was held constant at 160 MPa. For (d)–(i), $L_{\text{H}_2\text{O}}$ was 2 wt %. For (a)–(c) and (g)–(i), L_{fO_2} was QFM + 1. The grey points are all literature glass data for eruptions in the last 15 kyr. This figure represents a selection of all rhyolite-MELTS models run; each intensive parameter was evaluated against the full range of the remaining two.

observed. These constraints lead to higher RMSE for models with $L_{\text{H}_2\text{O}}$ outside 2–3 wt % (Fig. 5a, d and g). For the northern/eastern and western caldera eruptions, the natural glass compositions are best reproduced by crystallisation with 2 wt % $L_{\text{H}_2\text{O}}$, whereas the central caldera eruptions are best reproduced with a higher $L_{\text{H}_2\text{O}}$ of 3 wt %.

The best-fit $L_{\text{H}_2\text{O}}$ for each volcano-tectonic setting (2–3 wt %) are consistent with previous measurements of mafic melt inclusion H_2O concentrations (Webster et al., 2003; Cannatelli et al., 2007; Mangiacapra et al., 2008; Stock et al., 2018), those determined experimentally (Perinelli et al., 2019) and $L_{\text{H}_2\text{O}}$ values used in previous thermodynamic modelling of Campi Flegrei eruptions

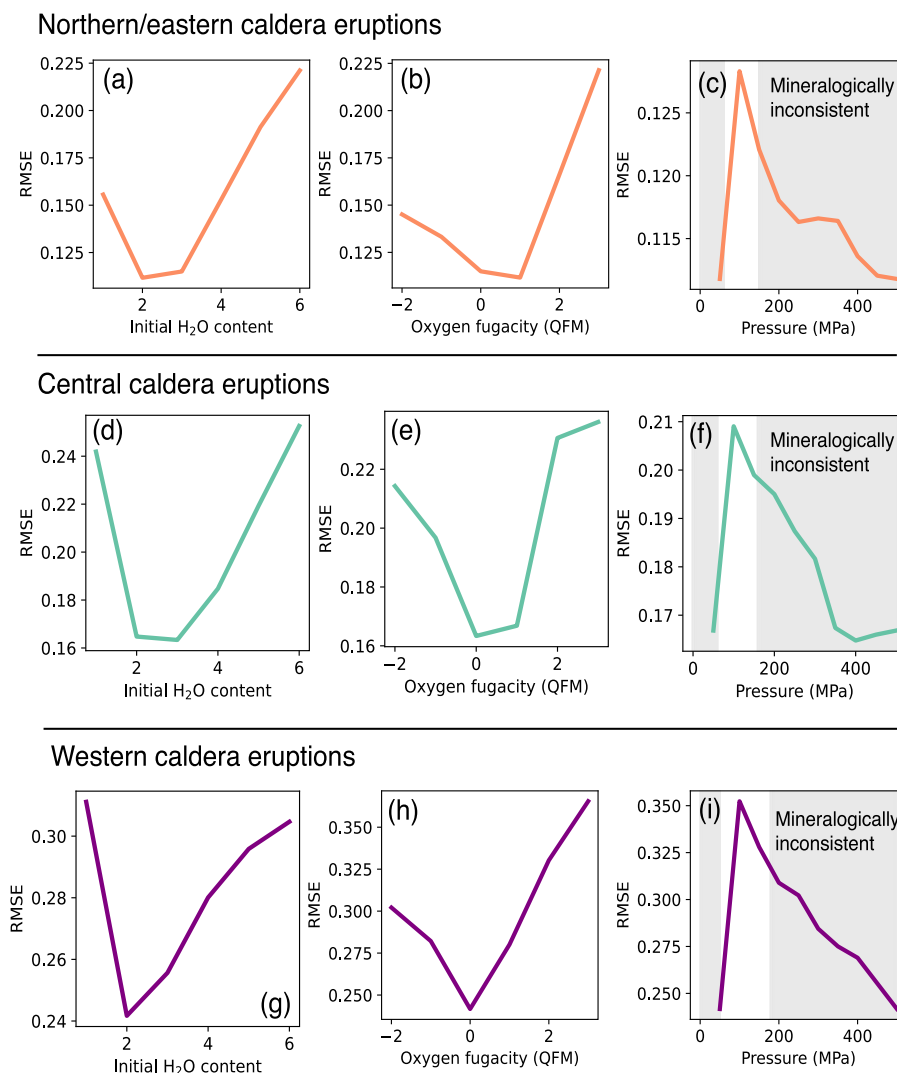


Fig. 5. The effect of varying each intensive parameter on the RMSE of the resulting rhyolite-MELTS model. For (a), (d) and (g), pressure and oxygen fugacity are held constant at the best-fit conditions for the tectonic group and the initial H₂O content is varied. For (b), (e) and (h), H₂O content and pressure are held constant and oxygen fugacity is varied. For (c), (f) and (i), H₂O content and oxygen fugacity are both held constant and pressure is varied. The grey-shaded regions in (c), (f), (i) indicate pressures at which rhyolite-MELTS predicts the crystallisation of phases which are not observed in natural Campi Flegrei rocks (muscovite, garnet, leucite).

Table 2: Best-fit FC storage conditions and assimilant compositions and quantities for each tectonic setting as defined by the lowest RMSE between rhyolite-MELTS models and the literature glass data

Best-fit	Northern/eastern caldera eruptions	Central caldera eruptions	Western caldera eruptions
Pressure (MPa)	110	140	160
Initial water content (wt %)	2	3	2
Oxygen fugacity (log units relative to the quartz-fayalite-magnetite buffer)	1	0	0
Assimilant composition	Palaeozoic basement	Syenite	Syenite
Amount (% of total mass of magma)	10	30	30
Normalised RMSE (FC)	0.142	0.227	0.377
Normalised RMSE (AFC)	0.118	0.114	0.206

(Bohrson et al., 2006; Fowler et al., 2007; Cannatelli, 2012; Stock et al., 2016). Forni et al. (2018) assessed the H₂O contents of melts in equilibrium with late-crystallising K-feldspar were higher than those of near liquidus melts (i.e. prior significant crystallisation of anhydrous minerals), and also suggested that the H₂O content of Campi Flegrei magmas increased over the past 15 ka, from 0.5–

3.5 wt % in the Epoch 1 Minopoli 1 and 2 eruptions to 3–6 wt % in the Epoch 3 Astroni and Monte Nuovo eruptions. However, their study only included a small number (12) of eruptions from the past 15-kyr and did not consider the possibility for a spatial, rather than temporal, correlation. As earlier eruptions generally occurred along the caldera rim and migrated towards the centre

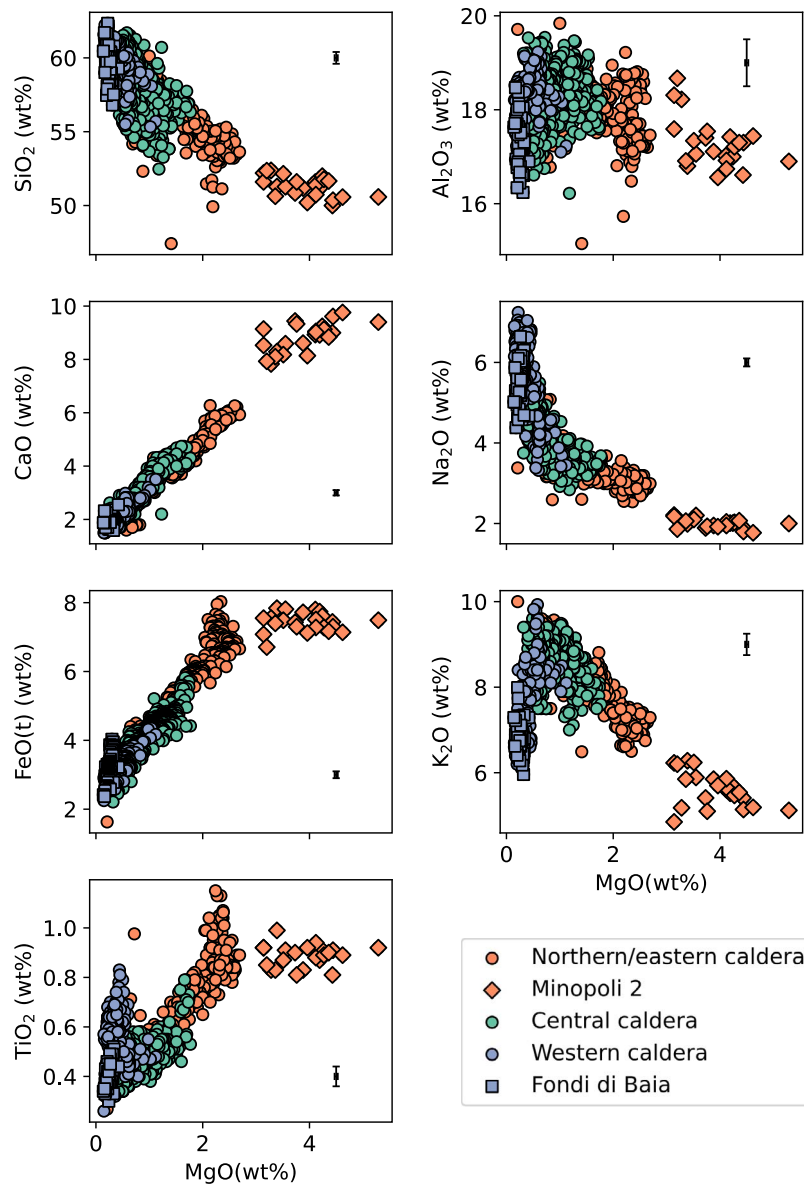


Fig. 6. Harker diagrams of literature glass data for Campi Flegrei eruptions in the last 15 kyr. Points are coloured by tectonic group as illustrated in Fig. 1. Error bars show representative 2 SD error from EPMA analysis from Smith *et al.* (2011). Glass data were compiled from GEOROC, and studies are referenced in Literature data. Minopoli 2 eruption, which forms a distinct high-MgO group, are shown with diamond markers and data from the Fondi di Baia eruption, which is discussed in the *Assimilation at Fondi di Baia* section, are shown with square markers.

of the caldera over time (Smith *et al.*, 2011), their results are equally compatible with differences in L_{H_2O} between volcano-tectonic groups. Eruptions from vents on the caldera rim (e.g. Minopoli 1 and 2, Soccavo 4) were identified by Forni *et al.* (2018) as having lower H_2O contents than eruptions in the central caldera (e.g. Astroni, Agnano-Monte Spina). The eruption of Monte Nuovo, in the western caldera but with the highest H_2O content in the last 15 kyr, is the exception, which may be related to extensive fractionation at low temperatures.

The differences in best-fit L_{H_2O} between our volcano-tectonic groups could reflect changes in the H_2O content of near-primitive mantle melts feeding Campi Flegrei eruptions in different parts of the caldera system. However, despite their different structural setting, post-15 kyr Campi Flegrei eruptions are relatively closely spaced (e.g. ~ 1 km between some central and caldera rim vents) relative to a whole arc or ocean island scale, and L_{H_2O} variations would need to occur on significantly shorter length scales than

any previously reported mantle heterogeneity (Kelemen *et al.*, 2003; Gibson *et al.*, 2012; Sims *et al.*, 2013). Consequently, we discount mantle heterogeneity as the potential source for variable L_{H_2O} across the caldera. Instead, we suggest that variations in L_{H_2O} between magmas in different volcano-tectonic settings result from interaction with hydrothermal water; such magma-fluid interaction has been suggested previously for Campi Flegrei eruptions on the basis of trace element and isotopic variation (Villemant, 1988; Civetta *et al.*, 1991). Although our approach cannot determine whether hydrothermal interaction and magma hydration genuinely occurred above the liquidus (i.e. as opposed to after some crystallisation), addition of water to the melt must have occurred at high enough temperatures and melt fractions to impact the crystallising phase assemblage. Campi Flegrei currently has a highly active hydrothermal system focused around Solfatara, in the central caldera (Troiano *et al.*, 2022) with geological evidence that this has persisted over the past 15 kyr

(Isaia *et al.*, 2009). While the main hydrothermal aquifer beneath Campi Flegrei is currently within the shallow crust (2–3 km; Troiano *et al.*, 2022) above the main zone of magma storage (see below), the eruption of hydrothermally altered syenitic lithics (Fedele *et al.*, 2006; Gebauer *et al.*, 2014) suggests that fluids may be present at significantly greater depths; this is supported by recent magnetotelluric imaging that shows a volatile-rich zone extending to ~8 km (Isaia *et al.*, 2025).

Oxygen fugacity

Varying L_{fO_2} between QFM – 2 and QFM + 3 has a significant effect on the predicted liquid line of descent, particularly for FeO and SiO₂, which are most impacted by changes in spinel stability (Fig. 4e). Under more oxidising conditions, spinel group minerals stabilise at higher temperatures resulting in lower FeO and higher SiO₂ concentrations in the residual melt, as observed in experimental studies (Hill & Roeder, 1974; Fisk & Bence, 1980). For $L_{fO_2} > \text{QFM} + 1$, the predicted liquid line of descent for FeO significantly deviates from that measured in natural Campi Flegrei glasses, leading to higher RMSE for these models (Fig. 5b, e and h). For the central and western caldera eruptions, the natural glass compositions are best reproduced by crystallisation with L_{fO_2} at the QFM buffer; the northern/eastern caldera eruptions are best reproduced with L_{fO_2} QFM + 1.

Our best-fit L_{fO_2} of QFM to QFM + 1 suggests that the liquidus oxidation state of the magma is broadly similar across the caldera. Although we do not fix fO_2 to a buffering reaction below the liquidus in our models (as these reactions very rarely occur in nature; Anenburg & O'Neill, 2019), our best-fit L_{fO_2} range agrees well with previous thermodynamic modelling (Bohrson *et al.*, 2006; Fowler *et al.*, 2007; Cannatelli, 2012) and experimental studies (Fabrizio & Carroll, 2008), which have consistently reproduced the phase assemblage of Campi Flegrei erupted products with fO_2 buffered between QFM and QFM + 1.8 (close to Ni-NiO + 1 at magmatic conditions, Frost, 1991). Our results are also consistent with fO_2 estimates for the Campanian Ignimbrite calculated by spinel-melt oxybarometry (QFM + 1; Forni *et al.*, 2016).

Pressure

Varying pressure in the range 50–500 MPa has minimal effect on the liquid line of descent of all the major oxides (Fig. 4g–i), with the predicted concentrations of major oxides varying by <1% at any given MgO concentration or temperature across the entire range of pressures (where other intrinsic variables are constant). Therefore, our RMSE statistical method is not an accurate discriminator of best-fit pressure. Egger (1972) experimentally demonstrated that plagioclase stability is strongly sensitive to the equilibrium melt H₂O content but relatively insensitive to pressure, with melt-H₂O sensitivity also observed in erupted products at Stromboli by Landi *et al.* (2004). As plagioclase is a major crystallising phase in Campi Flegrei magmas (Isaia *et al.*, 2004; Piochi *et al.*, 2005; Stock *et al.*, 2018), this may partly explain the models' relative insensitivity to pressure variations. However, while the overall liquid line of descent predicted by rhyolite-MELTS is relatively pressure insensitive, the mineral phase assemblage does vary close to the solidus and allows for some constraint on the most probable storage conditions. Our models predict that relatively late-stage muscovite and garnet will crystallise in Campi Flegrei magmas at pressures >200 MPa and that ~7% of leucite will precipitate at pressures <70 MPa (Figs 3 and S4). Muscovite and garnet have never been reported in any Campi Flegrei eruption products and leucite has only been observed rarely in low concentration (Isaia *et al.*, 2004; Smith *et al.*, 2011; Stock *et al.*, 2018);

hence, these pressures likely represent unrealistic magma storage conditions. Despite our models run at intermediate pressures having the highest RMSE when comparing predicted liquid lines of descent to natural glasses (i.e. RMSEs decrease at both low and high pressures; Fig. 5c, f and i), this mineralogical disparity constrains storage pressures to the range 70–200 MPa. Within this range, the best-fit pressure for each volcano-tectonic group can be determined approximately by the lowest RMSE for SiO₂, which is the most sensitive to pressure variations. For the northern/eastern caldera eruptions, the natural glass compositions are best reproduced by crystallisation at 110 MPa, for the central caldera eruptions the best-fit pressure increases to 140 MPa and is highest for the western caldera eruptions, at 160 MPa.

Given an average Campanian crustal density of 2.3 g cm⁻³ after Rosi & Sbrana (1987), our approximated crystallisation pressures correspond to magma storage depths in the range ~5–7 km. This broadly agrees with previous phase equilibria investigations at Campi Flegrei, which visually identified that the compositions of natural samples were best reproduced by models run at pressures equivalent to 6–12 km (150–300 MPa; Bohrson *et al.*, 2006; Fowler *et al.*, 2007; Cannatelli, 2012). Despite the inherent insensitivity of our method, our crystallisation depth estimate also agrees reasonably with independent petrological and geophysical constraints on the structure of the Campi Flegrei magmatic system, which predict the main magma storage region to be located at ~7–8 km (Zollo *et al.*, 2008; Stock *et al.*, 2018; Petrelli *et al.*, 2023; Isaia *et al.*, 2025). Critically, our depth estimates are not consistent with shallower crystallisation at 3–4 km, which corresponds with the depth of the current deformation source (Woo & Kilburn, 2010; Amoroso *et al.*, 2014; D'Auria *et al.*, 2015) and most recent seismicity (Scotto di Uccio *et al.*, 2024). This shallow unrest has previously been linked to fluid migration in the active hydrothermal system beneath Campi Flegrei (Troiano *et al.*, 2011; Chiodini *et al.*, 2012, 2015b) and may occur at the same depth as small/ephemeral sill intrusions (Stock *et al.*, 2018). Rather, our data support the majority of magma storage and crystallisation occurring in the mid-lower crust.

Volcano-tectonic controls on assimilation

Rhyolite-MELTS FC models can produce best-fit liquid lines of descent which correlate reasonably with natural glass compositions for some major oxides (e.g. CaO, FeO; Figs 6, S18–S20) and there is a good agreement between the modelled phase assemblages and those observed in Campi Flegrei erupted products. However, models fail to reproduce natural glass compositions for other major oxides under any set of intensive parameters. For example, modelled Al₂O₃ concentrations are consistently higher than in natural glasses, whereas SiO₂ concentrations are consistently lower (Fig. 7). While models are able to reproduce the K₂O composition of erupted glasses from the northern/eastern and central caldera volcano-tectonic groups, the lower K₂O concentration of the western caldera eruptions is not reproduced by any of our FC models (Fig. S20). These discrepancies suggest that assimilation may play a role in controlling the Campi Flegrei liquid line of descent, where addition of a contaminant could improve the fit between our model outputs and natural glass compositions.

Despite evidence for extensive limestone contamination at Vesuvius (~25 km east of Campi Flegrei; Del Moro *et al.*, 2001; Iacono Marziano *et al.*, 2008) and previous authors interpreting this as a potential contaminant of Campi Flegrei magmas (Iacono Marziano *et al.*, 2008; Pappalardo & Mastrolorenzo, 2012) addition of limestone does not significantly improve the fit between

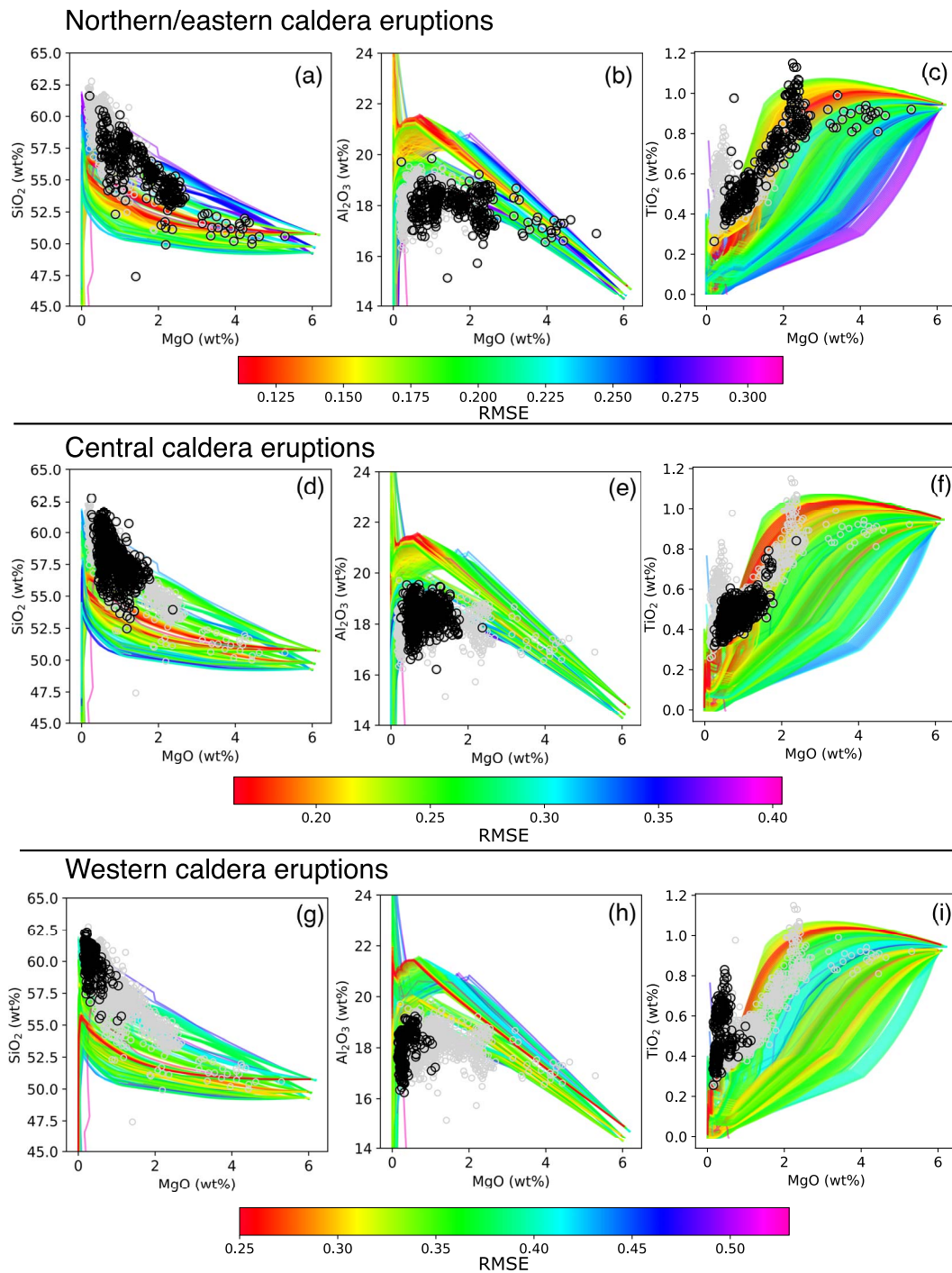


Fig. 7. Results of all rhyolite-MELTS models of fractional crystallisation. Grey points represent all literature glass data for eruptions in the last 15 kyr and black points are literature glass data for the tectonic group indicated. Each line represents the liquid line of descent predicted by rhyolite-MELTS for a parental magma cooling and crystallising under a given pressure, initial H₂O content and oxygen fugacity. Each model is coloured according to the RMSE value indicating the goodness-of-fit between the model and natural data; red indicates a better fit, blue/purple indicates a worse fit. See section “Statistical determination of best-fit storage conditions” for description of RMSE calculation, RMSE is an average of all major oxides. Plots of the other major oxides that are not shown in this figure are included in the Supplementary Material Figs S18–S20.

predicted and observed liquid lines of descent in post-15 ka volcano-tectonic groups relative to FC alone. This is reflected in limestone contamination producing only a very minor decreases in the RMSE between modelled and observed glass compositions; increasing quantities of a limestone assimilant lowers the melt SiO₂ concentration and increases CaO, forcing the predicted liquid line of descent for these elements away from the observed compositions of all volcano-tectonic groups (Figs S6, S10 and S14). At

$M_a/M_m > 0.05$, limestone-contaminated models predict the crystallisation of garnet, which has never been observed in natural Campi Flegrei samples. Hence, in contrast with Vesuvius, our models clearly show that limestone is not a contaminant in Campi Flegrei (with the possible exception of the Fondi di Baia eruption, see below).

Syn-orogenic wedge-top deposits have previously been identified as a potential contaminant of Campi Flegrei magmas, based

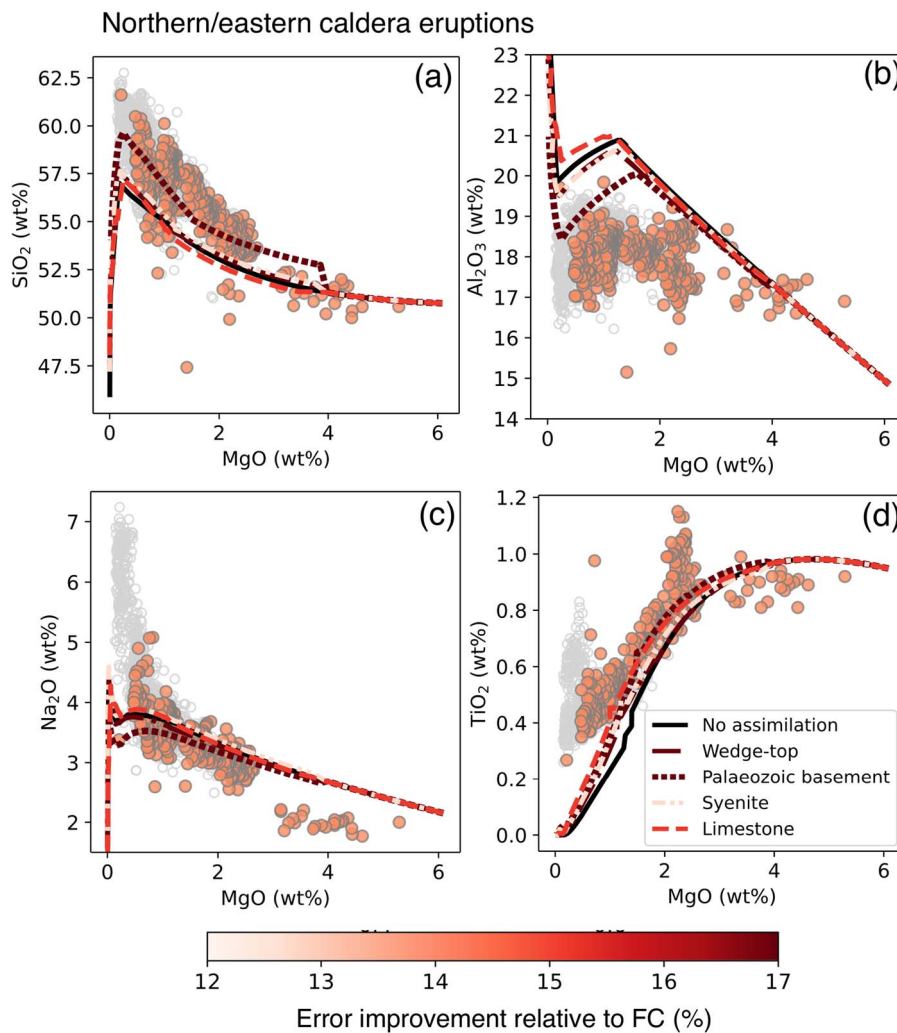


Fig. 8. Results of rhyolite-MELTS models of assimilation-fractional crystallisation for the northern/eastern caldera group eruptions. Line styles indicate different assimilant compositions, the solid black line shows the best-fit FC model for the northern/eastern caldera eruptions. For each assimilant composition, the amount of assimilant, which led to the largest improvement in model fit compared to the FC-only model, is plotted. The line colour refers to the percentage improvement of RMSE relative to the best-fit FC-only model, pale red indicates less improvement to darker red, which indicates the most improvement. Fit was calculated using normalised RMSE, as for FC models. Pale grey circles represent all literature glass data for eruptions in the last 15 kyr, orange-filled circles represent literature glass data from the northern/eastern caldera group eruptions. Assimilant was added *en masse* at 1100 °C. Full results of AFC modelling for the eastern caldera group eruptions are included in Figs S6–S9

on their occurrence in the shallow crust within the Neapolitan area (D'Erasmus, 1931; Bernasconi *et al.*, 1981; Sollevanti, 1983). Where large amounts of wedge-top deposits ($M_a/M_m = 0.2\text{--}0.3$) are added to rhyolite-MELTS AFC models, predicted liquid lines of descent have significantly higher SiO_2 and lower Na_2O , FeO and TiO_2 contents than are observed in natural Campi Flegrei glasses, increasing the RMSE relative to simple FC models (Figs S7, S11 and S15). Addition of small amounts of wedge-top deposits leads to K_2O enrichment in the melt at low temperatures as sanidine crystallisation is suppressed. While this mineralogical change is inconsistent with observations of natural samples (which all contain sanidine; Smith *et al.*, 2011) and negates this assimilation source, minor wedge-top deposits contamination lowers the predicted melt Al_2O_3 content compared to FC models, which improves the overall fit between the observed and modelled liquid line of descent and reduces the RMSE in all volcano-tectonic groups, especially for very small amounts of contamination ($M_a/M_m = 0.05$; Figs 8–10).

Long-lived volcanic systems are often thought to be underlain by large volumes of crystalline residue (mush), which fractionated

during magmatic evolution but remained in the crust as their accompanying liquids were evacuated during eruptions; in silicic systems, this crystalline restite has a syenitic or granitic composition (Bachmann & Huber, 2016; Cashman *et al.*, 2017; Edmonds *et al.*, 2019; Horn *et al.*, 2022). Campi Flegrei has been active for >300 kyr (De Vivo *et al.*, 2001; Rolandi *et al.*, 2003; Di Vito *et al.*, 2008), and the presence of a sub-volcanic crystalline residue is attested by the presence of syenitic lithics, with previous thermodynamic studies suggesting that syenite assimilation impacted the composition of melts erupted during the Campanian Ignimbrite (Fowler *et al.*, 2007). In our models, assimilation of large proportions of syenite ($M_a/M_m = 0.3$) increases the SiO_2 content of the liquid and reduces the Al_2O_3 concentration (due to greater proportions of feldspar crystallising), improving the correlation between the modelled liquid line of descent and natural glass compositions. The RMSE, averaged across all major elements, is also reduced relative to simple FC models in all volcano-tectonic environments (Figs S9, S13 and S17). However, while predicted liquid lines of descent for syenite-contaminated magmas closely match the compositions of erupted glasses for the central caldera

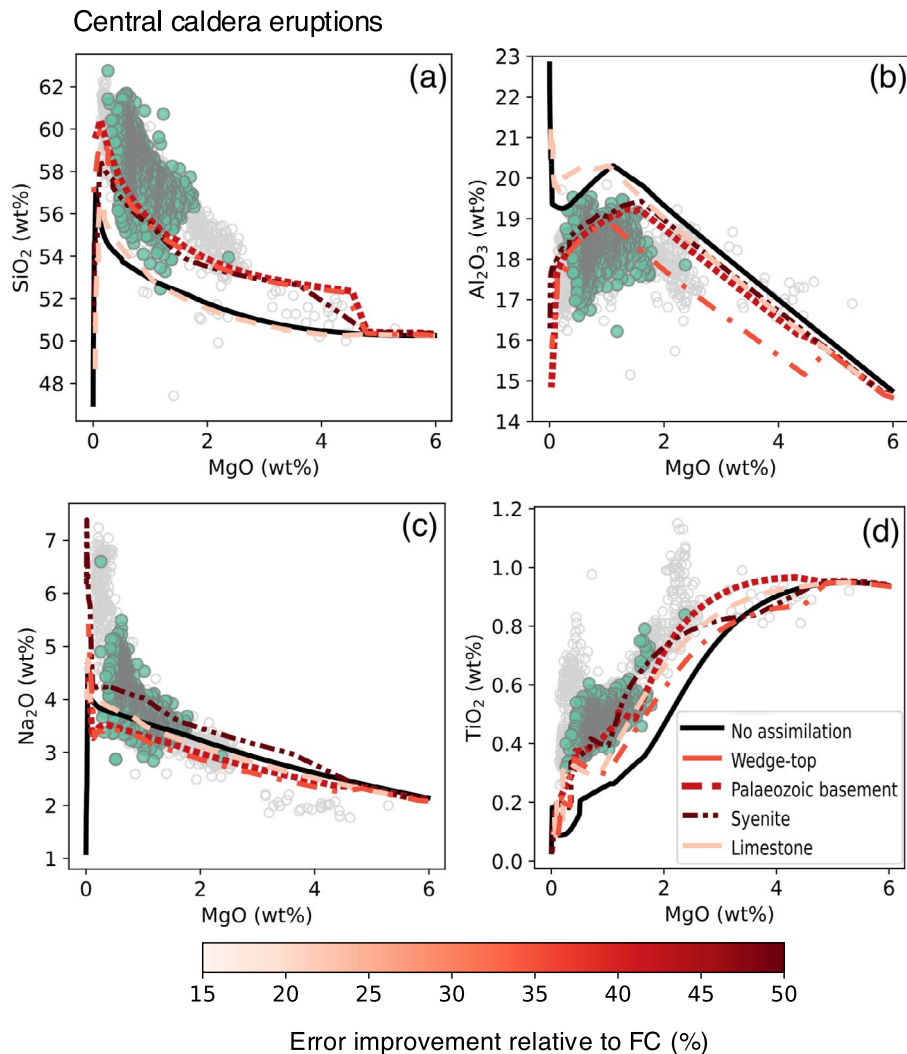


Fig. 9. Results of rhyolite-MELTS models of assimilation-fractional crystallisation for the central caldera group eruptions. The colouring and line style of each rhyolite-MELTS model is as described for Fig. 7. Pale grey circles represent all literature glass data for eruptions in the last 15 kyr, green-filled circles represent literature glass data from the central caldera group eruptions. Full results of AFC modelling for the central caldera group eruptions are included in Figs S10–S13

and western caldera eruptions, modelled Na_2O concentrations markedly deviate from the observed concentrations at low temperatures for the northern/eastern caldera eruptions, predicting much higher Na_2O concentrations than are observed.

Much of the central Italy is underlain by Palaeozoic metamorphic basement, predominantly comprising low-grade to granulite-facies metamorphic rocks, which formed during the Variscan orogeny (Caggianelli & Prosser, 2001). While the basement depth directly beneath Campi Flegrei remains poorly constrained geophysically and these Palaeozoic rocks have not been intersected in borehole records (AGIP, 1987), seismic datasets reveal relatively shallow basement (≥ 4 km; Battaglia *et al.*, 2008; Berrino *et al.*, 2008) beneath Campi Flegrei and these have been suggested as potential source of isotopic contamination in Campi Flegrei magmas (Pappalardo *et al.*, 2002). Our models predict quartz saturation at relatively low temperatures with large amounts ($M_a/M_m > 0.2$) of Palaeozoic metapelitic contamination and the absence of quartz in natural Campi Flegrei eruption products (Isaia *et al.*, 2004; Smith *et al.*, 2011) makes this an unlikely assimilation scenario. However, our models do not predict quartz saturation with smaller amounts of Palaeozoic metamorphic con-

tamination ($M_a/M_m < 0.2$) but do produce higher melt SiO_2 contents and lower Al_2O_3 contents than simple fractional crystallisation, improving calculated RMSEs for all volcano-tectonic environments (Figs S8, S13 and S17). While syenite contamination returns lower RMSEs for the central and western caldera eruptions (of 0.11 and 0.21, representing 50 and 45% improvements, respectively, in the RMSE compared to FC alone), Palaeozoic metamorphic assimilation generates a lower RMSE overall for the northern/eastern caldera eruptions (of 0.12, representing a 17% improvement on FC alone). These more mafic eruptions, from vents along the caldera rim faults, were generally earlier in the last 15 kyr, following the NYT eruption. This suggests earlier eruptions ascended from depth where they encountered the metamorphic basement before erupting along the caldera ring faults, whereas the later eruptions, in the central caldera, stalled in the crust and interacted with residual syenite before eruption.

A summary of best-fit AFC model outputs for each volcano-tectonic group (i.e. lowest RMSE) is shown in Figs 8–10 and Tables S7–S9. In all volcano-tectonic settings, AFC models can produce liquid lines of descent which are closer to natural glass compositions than simple FC models. However, the nature of

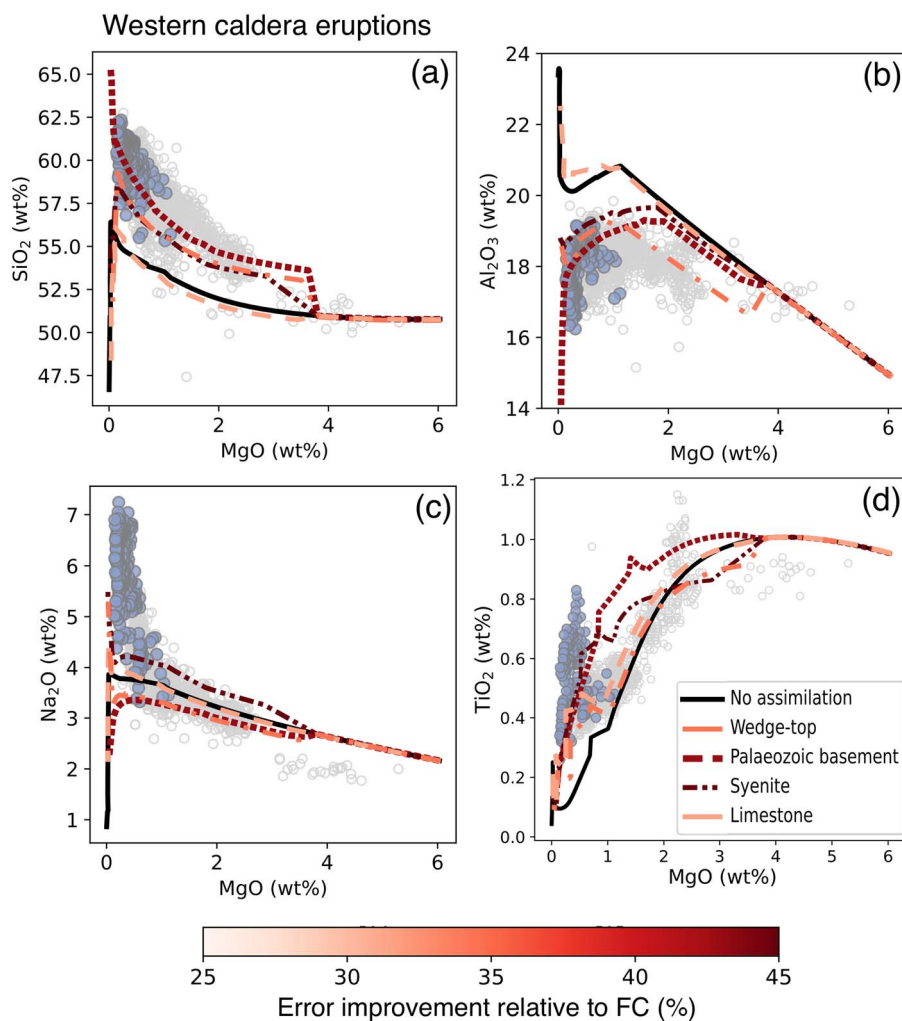


Fig. 10. Results of rhyolite-MELTS models of assimilation-fractional crystallisation for the western caldera group eruptions. The colouring and line style of each rhyolite-MELTS model is as described for Fig. 7. Pale grey circles represent all literature glass data for eruptions in the last 15 kyr, purple-filled circles represent literature glass data from the western caldera group eruptions. Full results of AFC modelling for the western caldera group eruptions are included in Figs S14–S17

the assimilant source and extent of contamination in the best-fitting model varies between each group. For the northern/eastern caldera eruptions, the best-fit assimilation scenario is the addition of 0.05–0.1 M_a/M_o Palaeozoic metamorphic basement, which improves the fit of the model by ~17% compared to simple FC (Figs 8, S6 and S9). This is consistent with AFC models of isotopic and trace element variations in selected post-15 ka eruptions, which suggest ~1–12% crustal assimilation of Palaeozoic metamorphic basement would explain the observed compositional variations (Pappalardo *et al.*, 2002; D’Antonio *et al.*, 2007; Iovine *et al.*, 2018). For the central caldera eruptions, the best-fit assimilation scenario is addition 0.2–0.3 M_a/M_o syenitic material, which improves the model RMSE by ~49% relative to FC models (Figs 9 and S10–S13). This is the same for the western caldera eruptions; the best-fit assimilation scenario is 0.25–0.3 M_a/M_o of syenite, which produces a ~45% improvement compared to simple FC models (Figs 10 and S14–S17). Hence, our results suggest that post-15 kyr eruptions in different volcano-tectonic environments within the Campi Flegrei caldera not only underwent crystallisation under different intensive conditions but also interacted with different types of country rock material, consistent with the magnetotelluric imaging of Isaia *et al.* (2025), which suggests a transcrustal magmatic system in contact with

basement rock at its margins. Eruptions along the caldera rim faults at the northern and eastern margins of the system were able to ‘see’ and interact with Palaeozoic metamorphic basement at depth, prior to ascent and eruption, whereas eruptions from the centre of the caldera and along regional faults in the west of the caldera were stored within crystalline igneous material, left in the crust as a restitic residue during past eruptions.

Assimilation at Fondi di Baia

The eruption of Baia-Fondi di Baia at the beginning of Epoch 2 (~9.6 ka) was one of the most compositionally distinct events in the last 15 kyr, producing evolved melts from a vent located on a regional fault system on the west side of the caldera (Smith *et al.*, 2011; Pistolesi *et al.*, 2017; Vitale & Natale, 2023). While we have categorised it as a western caldera eruption based on its volcano-tectonic setting, the trace element compositions of Baia-Fondi di Baia glasses are distinct from all other post-15 ka Campi Flegrei eruptions, with low Ba and Sr concentrations and high Y, Nb, Nd and Th (Smith *et al.*, 2011). Previous studies have attributed this compositional deviation to mixing between distinct magma batches, which had separate AFC evolutionary histories; while Sr-isotopes suggest some amount of limestone contamination, this was ruled out based on the absence of significantly elevated

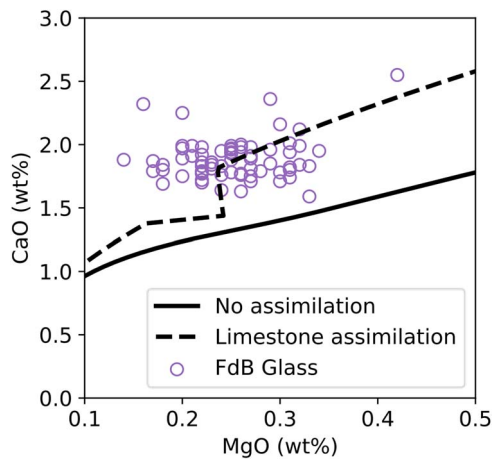


Fig. 11. Rhyolite-MELTS model of limestone assimilation compared to Fondi di Baia glass data (circles; literature data). Solid line is the result of the best-fit fractional crystallisation rhyolite-MELTS model for the western caldera eruptions group. Dashed line is the result of a rhyolite-MELTS model run at the same pressure (160 MPa), $L_{\text{H}_2\text{O}}$ (2 wt %) and L_{fO_2} conditions (at QFM buffer) with addition of 1% limestone.

CaO concentrations, with authors instead invoking assimilation of residual magma from the CI (Voloschina et al., 2018). However, our models suggest that in contrast to other eruptions in the west of the caldera, which are best reproduced by assimilation of crystalline restite, the addition of small amounts (0.01 M_3/M_0) of limestone to our best-fit FC model for the western caldera eruptions accurately reproduces the major element compositions of Baia-Fondi di Baia glasses, with the fit between the modelled liquid line of descent and natural glass compositions significantly improved for CaO, FeO and TiO_2 (other major oxides do not significantly change; Figs 11 and S21).

Although carbonate xenoliths have not previously been identified in Campi Flegrei eruption deposits (in contrast with Vesuvius; Fulignati et al., 2000; Del Moro et al., 2001; Gilg et al., 2001), Mesozoic carbonates have been suggested as a possible lithology underlying the volcano at shallow levels (Brocchini et al., 2001; Judenherc & Zollo, 2004; Battaglia et al., 2008; Zollo et al., 2008). Since Campi Flegrei caldera has been active for at least 300 kyr (De Vivo et al., 2001), any carbonate would have been progressively removed during the previous eruptions, whereas the younger Vesuvius magmatic system has only been active for the last 39 kyr (Scandone et al., 1991; Brocchini et al., 2001) and is at an earlier stage in its development where an extensive shallow carbonate basement remains. It is possible that the tectonic setting of Baia-Fondi di Baia, on the west of the caldera and situated on regional faults, may have enabled interaction between the magma feeding the eruption and more peripheral carbonate country rocks. Alternatively, hydrothermal calcite has been documented in both Campi Flegrei borehole samples (Chiodini et al., 2015a) and lithic fragments, including tuffaceous lithics recovered from Baia deposits (Buono et al., 2024). While we used an upper Jurassic–lower Cretaceous limestone as the assimilant in our models, sedimentary limestone and hydrothermal calcite would have comparable major element compositions, similarly impacting our modelled AFC liquid lines of descent; hence, we cannot discount this as an alternative Baia-Fondi di Baia assimilant source.

Volcano-tectonic controls on eruptive processes

Alongside compositional information, rhyolite-MELTS outputs predicted physical properties for evolving magmas (e.g. density,

viscosity) as well as information on the behaviour of magmatic volatiles; these properties vary between our best-fit models for each of our three volcano-tectonic groups (Fig. 12). H_2O behaves incompatibly, consistently increasing in concentration within the melt phase as the magma cools, but with a greater enrichment per unit temperature below the invariant point (temperature at which melt fraction drops and physical properties change over a short interval), likely due to enhanced crystallisation of anhydrous minerals (Fig. 12a). The volume fraction of exsolved H_2O coexisting with the magma increases dramatically around the invariant point for all tectonic settings, from ~10 vol % below to ~60 vol % above this temperature (Fig. 12b). This is consistent with other studies at Campi Flegrei (Fowler et al., 2007; Cannatelli, 2012; Stock et al., 2016) and elsewhere (e.g. Mount St. Helens, USA—Kent et al., 2007; Calbuco, Chile—Arzilli et al., 2019), which suggest that the dramatic increase in volatile content at low temperatures could trigger explosive eruptions. Stock et al. (2016) used the volatile content of apatite crystals and melt inclusions in Astroni 1 deposits to demonstrate the magma reservoir beneath Campi Flegrei remained volatile undersaturated until low temperatures, with volatile saturation likely triggering eruption on very short pre-eruptive timescales, perhaps days to months. Forni et al. (2018) suggest Monte Nuovo may also have been triggered by volatile saturation, which occurred in the decades before the eruption.

H_2O saturation controls the viscosity and density evolution in our best-fit models (Fig. 12c and d). The large increase in melt H_2O content below the invariant point leads to a rapid drop in both viscosity and density across all tectonic settings, consistent with the results of Fowler et al. (2007) and Cannatelli (2012). The inflection in viscosity from an initial increase as magma cools and becomes more SiO_2 rich to a rapid decrease as dissolved melt H_2O concentration increases occurs at slightly higher temperatures and higher maximum viscosities for the northern/eastern caldera eruptions (830 °C) than the western caldera or central caldera eruptions (815–820 °C; Fig. 12a), reflecting small temperature differences in the invariant point. Our models show that, despite small differences in the temperatures at which viscosity and density change dramatically, the increase in volume fraction of exsolved H_2O occurs late in magmatic evolution, at similar temperatures for all tectonic groups. While it remains possible that some eruptions were triggered externally (e.g. by recharge), our models validate the potential for eruption triggering by low temperature volatile saturation in all volcano-tectonic groups, despite differences in their pre-eruptive history (e.g. assimilation processes).

CONCLUSIONS

We have shown that rhyolite-MELTS modelling can be used to evaluate a wide range of potential magma storage conditions, determining which (if any) can produce observed phase compositions by fractional crystallisation. Building on the statistical test proposed by Gleeson et al. (2017) to quantitatively evaluate which model best reproduces natural samples, we show that magma storage before eruptions of Campi Flegrei in the last 15 kyr was most likely at pressures of 110 to 160 MPa (corresponding to depths of ~5–7 km), with a parental magma with $L_{\text{H}_2\text{O}}$ of 2–3 wt % and an L_{fO_2} near the QFM buffer (QFM to QFM + 1). Eruptions from vents in the centre of the caldera likely had higher melt H_2O contents (3 wt %) compared to those erupted at vents along caldera rim faults or regional faults in the west of the caldera (2 wt %), possibly due to interaction with crustal fluids.

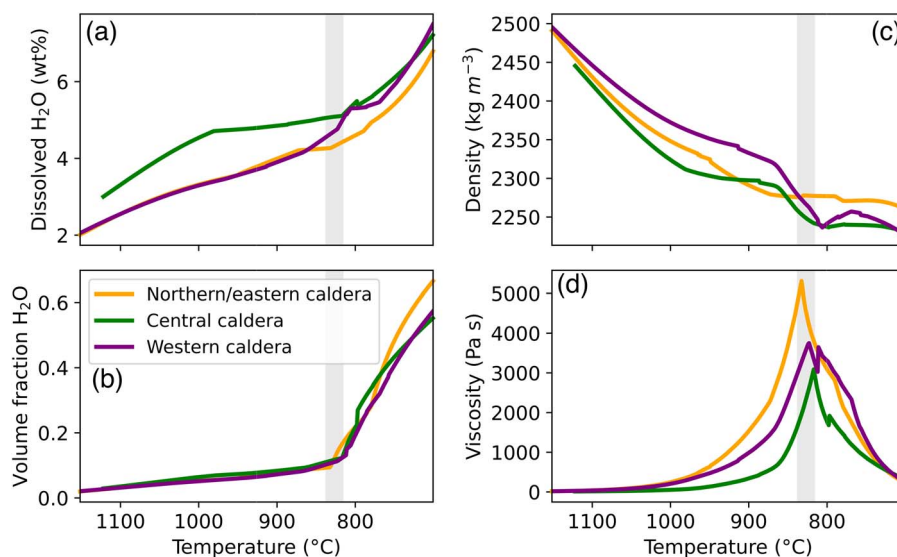


Fig. 12. Variation of melt physical properties along the liquid line of descent as predicted by the best-fit rhyolite-MELTS model for each tectonic group. Models were run at 110 MPa (northern/eastern caldera), 140 MPa (central caldera) and 160 MPa (western caldera) and models run at the same pressures showed no significant differences in physical properties displayed here (a) T vs dissolved H_2O content, (b) T vs density of melt, (c) T vs volume fraction of exsolved H_2O and (d) T vs melt viscosity. The vertical grey bar indicates the temperature range over which melt fraction drops and physical properties change over a short temperature interval (invariant temperature range).

We find that isobaric fractional crystallisation of a parental magma cannot fully reproduce the liquid line of descent recorded by natural samples under any realistic conditions. Instead, addition of a small amount of assimilated improves the fit of the models compared to observed compositions. For eruptions from vents along caldera ring faults in the east of the Campi Flegrei system, addition of 5–10% of metamorphic Palaeozoic basement leads to the biggest improvement in model fit compared to FC alone. For vents in the centre of the caldera and along regional faults in the west, addition of 30% syenite is the best-fit assimilation scenario. Our results indicate that the magmatic evolution of an eruption, in terms of storage and assimilation, correlates with the volcano-tectonic setting of its eruption vent. The central caldera eruptions were likely evolved within the crystalline syenitic remnants of previous eruptions, whereas those on the periphery of the caldera system ascended from depth along faults in contact with the surrounding metamorphic basement. As assimilation influences the compositional evolution of the magmas, which in turn impacts the magma's physical properties and the eruptive style, the vent location (in terms of the volcano-tectonic setting) needs to be considered in hazard forecasting.

SUPPLEMENTARY DATA

Supplementary data are available at *Journal of Petrology* online.

ACKNOWLEDGEMENTS

This research forms part of a PhD project of F.M.A funded by a Trinity College Dublin Provost's Award. Funding from a Trinity Trust Travel Grant awarded to F.M.A is acknowledged for fieldwork. F.M.A., M.J.S., V.C.S., R.I., S.V. and J.N. acknowledge funding from the INGV INSIDE OUT project and XRF data collection was supported by the Geological Survey Ireland-funded Earth Surface Research Laboratory in Trinity College Dublin. We thank Silvio Mollo, Samantha Tramontano and an anonymous reviewer for providing constructive feedback on the manuscript,

and Mary Reid and Georg Zellmer for their editorial handling and comments.

DATA AVAILABILITY

New geochemical data presented in this study have been deposited in EarthChem Library ([doi:10.60520/IEDA/113525](https://doi.org/10.60520/IEDA/113525)) and in the online supplementary material. Rhyolite-MELTS data underlying the study are available in the online supplementary material. A Python code to calculate RMSE between Rhyolite-MELTS outputs and natural glass data is available on GitHub at [doi:10.5281/zenodo.14900107](https://doi.org/10.5281/zenodo.14900107).

REFERENCES

- Acocella, V. (2010). Evaluating fracture patterns within a resurgent caldera: Campi Flegrei, Italy. *Bulletin of Volcanology* **72**, 623–638. <https://doi.org/10.1007/s00445-010-0347-x>.
- Agip (1987). Geologia e geofisica del sistema geotermico dei Campi Flegrei. *Technical report Settore Esplor* 1–23.
- Albert, P., Giaccio, B., Isaia, R., Costa, A., Niespolo, E. M., Nomade, S., Pereira, A., Renne, P. R., Hinchliffe, A., Mark, D. F., Brown, R. J. & Smith, V. C. (2019). Evidence for a large-magnitude eruption from Campi Flegrei caldera (Italy) at 29 ka. *Geology* **47**, 595–599. <https://doi.org/10.1130/G45805.1>.
- Amoruso, A., Crescentini, L., Sabbetta, I., De Martino, P., Obrizzo, F. & Tammaro, U. (2014). Clues to the cause of the 2011–2013 Campi Flegrei caldera unrest, Italy, from continuous GPS data. *Geophysical Research Letters* **41**, 3081–3088. <https://doi.org/10.1002/2014GL059539>.
- Anderson, A. T., Newman, S., Williams, S. N., Druitt, T. H., Skirius, C. & Stolper, E. (1989). H_2O , CO_2 , Cl , and gas in Plinian and ash-flow bishop rhyolite. *Geology* **17**, 221–225. [https://doi.org/10.1130/0091-7613\(1989\)017<0221:HOCCAG>2.3.CO;2](https://doi.org/10.1130/0091-7613(1989)017<0221:HOCCAG>2.3.CO;2).
- Anenburg, M. & O'Neill, H. S. C. (2019). Redox in magmas: comment on a recent treatment of the Kaiserstuhl Volcanics (Braunger et al., *Journal of Petrology*, 59, 1731–1762,

- 2018) and some other misconceptions. *Journal of Petrology* **60**, 1825–1832.
- Annen, C., Blundy, J. D., Leuthold, J. & Sparks, R. S. J. (2015). Construction and evolution of igneous bodies: towards an integrated perspective of crustal magmatism. *Lithos* **230**, 206–221. <https://doi.org/10.1016/j.lithos.2015.05.008>.
- Antoshechkina, P. M. & Ghiorsio, M. S. (2018). MELTS for MATLAB: a new educational and research tool for computational thermodynamics. *AGU Fall Meeting Abstracts*, ED44B-23.
- Arienzo, I., Moretti, R., Civetta, L., Orsi, G. & Papale, P. (2010). The feeding system of Agnano–Monte Spina eruption (Campi Flegrei, Italy): dragging the past into present activity and future scenarios. *Chemical Geology* **270**, 135–147. <https://doi.org/10.1016/j.chemgeo.2009.11.012>.
- Arienzo, I., Heumann, A., Wörner, G., Civetta, L. & Orsi, G. (2011). Processes and timescales of magma evolution prior to the Campanian ignimbrite eruption (Campi Flegrei, Italy). *Earth and Planetary Science Letters* **306**, 217–228. <https://doi.org/10.1016/j.epsl.2011.04.002>.
- Arienzo, I., Mazzeo, F. C., Moretti, R., Cavallo, A. & D'Antonio, M. (2016). Open-system magma evolution and fluid transfer at Campi Flegrei caldera (southern Italy) during the past 5ka as revealed by geochemical and isotopic data: the example of the Nisida eruption. *Chemical Geology* **427**, 109–124. <https://doi.org/10.1016/j.chemgeo.2016.02.007>.
- Arzilli, F., Morgavi, D., Petrelli, M., Polacci, M., Burton, M., Di Genova, D., Spina, L., La Spina, G., Hartley, M. E., Romero, J. E., Fellowes, J., Diaz-Alvarado, J. & Perugini, D. (2019). The unexpected explosive sub-Plinian eruption of Calbuco volcano (22–23 April 2015; southern Chile): triggering mechanism implications. *Journal of Volcanology and Geothermal Research* **378**, 35–50. <https://doi.org/10.1016/j.jvolgeores.2019.04.006>.
- Astbury, R. L., Petrelli, M., Ubide, T., Stock, M. J., Arienzo, I., D'Antonio, M. & Perugini, D. (2018). Tracking plumbing system dynamics at the Campi Flegrei caldera, Italy: high-resolution trace element mapping of the Astroni crystal cargo. *Lithos* **318–319**, 464–477. <https://doi.org/10.1016/j.lithos.2018.08.033>.
- Bachmann, O. & Huber, C. (2016). Silicic magma reservoirs in the Earth's crust. *American Mineralogist* **101**, 2377–2404. <https://doi.org/10.2138/am-2016-5675>.
- Balbone-Boissard, H., Boudon, G., Zdanowicz, G., Orsi, G., Webster, J. D., Civetta, L., D'Antonio, M. & Arienzo, I. (2024). The space-time architecture variation of the shallow magmatic plumbing systems feeding the Campi Flegrei and Ischia volcanoes (southern Italy) from halogen constraints. *American Mineralogist* **109**, 977–991. <https://doi.org/10.2138/am-2022-8883>.
- Battaglia, J., Zollo, A., Virieux, J. & Iacono, D. D. (2008). Merging active and passive data sets in traveltimes tomography: the case study of Campi Flegrei caldera (southern Italy). *Geophysical Prospecting* **56**, 555–573. <https://doi.org/10.1111/j.1365-2478.2007.00687.x>.
- Bernasconi, A., Bruni, P., Gorla, L., Principe, C. & Sbrana, A. (1981). Risultati preliminari dell'esplorazione geotermica profonda nell'area vulcanica del Somma-Vesuvio. *Rendiconti Della Società Geologica Italiana* **4**, 237–240.
- Berrino, G., Corrado, G. & Riccardi, U. (2008). Sea gravity data in the Gulf of Naples. A contribution to delineating the structural pattern of the Phlegraean Volcanic District. *Journal of Volcanology and Geothermal Research* **175**, 241–252. <https://doi.org/10.1016/j.jvolgeores.2008.03.007>.
- Bevilacqua, A., Isaia, R., Neri, A., Vitale, S., Aspinall, W. P., Bisson, M., Flandoli, F., Baxter, P. J., Bertagnini, A., Ongaro, T. E., Iannuzzi, E., Pistolesi, M. & Rosi, M. (2015). Quantifying volcanic hazard at Campi Flegrei caldera (Italy) with uncertainty assessment: 1. Vent opening maps. *Journal of Geophysical Research: Solid Earth* **120**, 2309–2329. <https://doi.org/10.1002/2014JB011775>.
- Bevilacqua, A., Flandoli, F., Neri, A., Isaia, R. & Vitale, S. (2016). Temporal models for the episodic volcanism of Campi Flegrei caldera (Italy) with uncertainty quantification. *Journal of Geophysical Research: Solid Earth* **121**, 7821–7845. <https://doi.org/10.1002/2016JB013171>.
- Bevilacqua, A., Neri, A., Bisson, M., Esposti Ongaro, T., Flandoli, F., Isaia, R., Rosi, M. & Vitale, S. (2017). The effects of vent location, event scale, and time forecasts on pyroclastic density current Hazard maps at Campi Flegrei caldera (Italy). *Frontiers in Earth Science* **5**. <https://doi.org/10.3389/feart.2017.00072>.
- Bianco, F., Capuano, P., Del Pezzo, E., De Siena, L., Maercklin, N., Russo, G., Vassallo, M., Virieux, J. & Zollo, A. (2022). Seismic and Gravity Structure of the Campi Flegrei Caldera, Italy. In: Orsi G., D'Antonio M. & Civetta L. (eds) *Campi Flegrei: A Restless Caldera in a Densely Populated Area*. Berlin, Heidelberg: Springer, pp.55–94.
- Blundy, J. & Cashman, K. (2008). Petrologic reconstruction of magmatic system variables and processes. *Reviews in Mineralogy and Geochemistry* **69**, 179–239. <https://doi.org/10.2138/rmg.2008.69.6>.
- Bohrson, W. A., Spera, F. J., Fowler, S. J., Belkin, H. E., De Vivo, B. & Rolandi, G. (2006). Petrogenesis of the Campanian Ignimbrite: Implications for crystal-melt separation and open-system processes from major and trace elements and Th isotopic data. In: Vivo, B. D. (ed.) *Developments in Volcanology*. Amsterdam: Elsevier, pp.249–288.
- Boschetti, F. O., Ferguson, D. J., Cortés, J. A., Morgado, E., Ebmeier, S. K., Morgan, D. J., Romero, J. E. & Silva Parejas, C. (2022). Insights into magma storage beneath a frequently erupting arc volcano (Villarrica, Chile) from unsupervised machine learning analysis of mineral compositions. *Geochemistry, Geophysics, Geosystems* **23**, e2022GC010333. <https://doi.org/10.1029/2022GC010333>.
- Brocchini, D., Principe, C., Castradori, D., Laurenzi, M. A. & Gorla, L. (2001). Quaternary evolution of the southern sector of the Campanian plain and early Somma-Vesuvius activity: insights from the Trecase 1 well. *Mineralogy and Petrology* **73**, 67–91. <https://doi.org/10.1007/s007100170011>.
- Buono, G., Caliro, S., Pappalardo, L. & Chiodini, G. (2024). Hydrothermal calcite formation in Campi Flegrei caldera, Italy: unraveling carbon sink processes in alkaline volcanic systems. *Scientific Reports* **14**, 16839. <https://doi.org/10.1038/s41598-024-67746-8>.
- Caggianelli, A. & Prosser, A. (2001). An exposed cross-section of late Hercynian upper and intermediate continental crust in the Sila nappe (Calabria, southern Italy). *Periodico di Mineralogia* **70**, 277–301.
- Calò, M. & Tramelli, A. (2018). Anatomy of the Campi Flegrei caldera using enhanced seismic tomography models. *Scientific Reports* **8**, 1–12. <https://doi.org/10.1038/s41598-018-34456-x>.
- Cannatelli, C. (2012). Understanding magma evolution at Campi Flegrei (Campania, Italy) volcanic complex using melt inclusions and phase equilibria. *Mineralogy and Petrology* **104**, 29–42. <https://doi.org/10.1007/s00710-011-0182-6>.
- Cannatelli, C., Lima, A., Bodnar, R., De Vivo, B., Webster, J. & Fedele, L. (2007). Geochemistry of melt inclusions from the Fondo Riccio and Minopoli 1 eruptions at Campi Flegrei (Italy). *Chemical Geology* **237**, 418–432. <https://doi.org/10.1016/j.chemgeo.2006.07.012>.
- Cannatelli, C., Doherty, A. L., Esposito, R., Lima, A. & De Vivo, B. (2016). Understanding a volcano through a droplet: a melt inclusion approach. *Journal of Geochemical Exploration* **171**, 4–19. <https://doi.org/10.1016/j.gexplo.2015.10.003>.
- Carracedo, J. C., Badiola, E. R., Guillou, H., Paterne, M., Scaillet, S., Torrado, F. J. P., Paris, R., Fra-Paleo, U. & Hansen, A. (2007). Eruptive

- and structural history of Teide volcano and rift zones of Tenerife, Canary Islands. *Geological Society of America Bulletin* **119**, 1027–1051. <https://doi.org/10.1130/B26087.1>.
- Carter, E. J., Stock, M. J., Beresford-Browne, A., Cooper, M. R., Raine, R. & Fereyrolles, A. (2024). Volcanic tempo driven by rapid fluctuations in mantle temperature during large igneous province emplacement. *Earth and Planetary Science Letters* **644**, 118903. <https://doi.org/10.1016/j.epsl.2024.118903>.
- Cashman, K. V., Sparks, R. S. J. & Blundy, J. D. (2017). Vertically extensive and unstable magmatic systems: a unified view of igneous processes. *Science* **355**. <https://doi.org/10.1126/science.aag3055>.
- Cassidy, M., Manga, M., Cashman, K. & Bachmann, O. (2018). Controls on explosive-effusive volcanic eruption styles. *Nature Communications* **9**, 2839. <https://doi.org/10.1038/s41467-018-05293-3>.
- Chiodini, G., Caliro, S., De Martino, P., Avino, R. & Gherardi, F. (2012). Early signals of new volcanic unrest at Campi Flegrei caldera? Insights from geochemical data and physical simulations. *Geology* **40**, 943–946. <https://doi.org/10.1130/G33251.1>.
- Chiodini, G., Pappalardo, L., Aiuppa, A. & Caliro, S. (2015a). The geological CO₂ degassing history of a long-lived caldera. *Geology* **43**, 767–770. <https://doi.org/10.1130/G36905.1>.
- Chiodini, G., Vandemeulebrouck, J., Caliro, S., D'Auria, L., De Martino, P., Mangiacapra, A. & Petrillo, Z. (2015b). Evidence of thermal-driven processes triggering the 2005–2014 unrest at Campi Flegrei caldera. *Earth and Planetary Science Letters* **414**, 58–67. <https://doi.org/10.1016/j.epsl.2015.01.012>.
- Ciarra, S. & Vitale, S. (2025). Orogenic evolution of the northern Calabria–southern Apennines system in the framework of the Alpine chains in the Central-Western Mediterranean area. *Geological Society of America Bulletin* **137**, 1143–1176. <https://doi.org/10.1130/B37474.1>.
- Civetta, L., Carluccio, E., Innocenti, F., Sbrana, A. & Taddeucci, G. (1991). Magma chamber evolution under the Phlegraean fields during the last 10 ka: trace element and isotope data. *European Journal of Mineralogy* **3**, 415–428. <https://doi.org/10.1127/ejm/3/2/0415>.
- Cole, J., Milner, D. & Spinks, K. (2005). Calderas and caldera structures: a review. *Earth-Science Reviews* **69**, 1–26. <https://doi.org/10.1016/j.earscirev.2004.06.004>.
- D'Antonio, M. (2011). Lithology of the basement underlying the Campi Flegrei caldera: Volcanological and petrological constraints. *Journal of Volcanology and Geothermal Research* **200**, 91–98. <https://doi.org/10.1016/j.jvolgeores.2010.12.006>.
- D'Antonio, M., Civetta, L., Orsi, G., Pappalardo, L., Piochi, M., Carandente, A., De Vita, S., Di Vito, M. & Isaia, R. (1999). The present state of the magmatic system of the Campi Flegrei caldera based on a reconstruction of its behavior in the past 12 ka. *Journal of Volcanology and Geothermal Research* **91**, 247–268. [https://doi.org/10.1016/S0377-0273\(99\)00038-4](https://doi.org/10.1016/S0377-0273(99)00038-4).
- D'Antonio, M., Tonarini, S., Arienzo, I., Civetta, L. & Di Renzo, V. (2007). Components and processes in the magma genesis of the Phlegraean Volcanic District, southern Italy. *Special Papers-Geological Society of America* **418**, 203. [https://doi.org/10.1130/2007.2418\(10\)](https://doi.org/10.1130/2007.2418(10)).
- D'Auria, L., Pepe, S., Castaldo, R., Giudicepietro, F., Macedonio, G., Ricciolino, P., Tizzani, P., Casu, F., Lanari, R., Manzo, M., Martini, M., Sansosti, E. & Zinno, I. (2015). Magma injection beneath the urban area of Naples: a new mechanism for the 2012–2013 volcanic unrest at Campi Flegrei caldera. *Scientific Reports* **5**, 13100. <https://doi.org/10.1038/srep13100>.
- D'Erasmo, G. (1931) *Studio geologico dei pozzi profondi della Campania*. Naples, Italy: Jovene.
- Danyushevsky, L. V., McNeill, A. W. & Sobolev, A. V. (2002). Experimental and petrological studies of melt inclusions in phenocrysts from mantle-derived magmas: an overview of techniques, advantages and complications. *Chemical Geology* **183**, 5–24. [https://doi.org/10.1016/S0009-2541\(01\)00369-2](https://doi.org/10.1016/S0009-2541(01)00369-2).
- De Siena, L., Del Pezzo, E. & Bianco, F. (2010). Seismic attenuation imaging of Campi Flegrei: evidence of gas reservoirs, hydrothermal basins, and feeding systems. *Journal of Geophysical Research: Solid Earth* **115**.
- De Vivo, B., Rolandi, G., Gans, P., Calvert, A., Bohrsen, W. A., Spera, F. & Belkin, H. (2001). New constraints on the pyroclastic eruptive history of the Campanian volcanic plain (Italy). *Mineralogy and Petrology* **73**, 47–65. <https://doi.org/10.1007/s007100170010>.
- Deino, A. L., Orsi, G., de Vita, S. & Piochi, M. (2004). The age of the Neapolitan yellow tuff caldera-forming eruption (Campi Flegrei caldera–Italy) assessed by ⁴⁰Ar/³⁹Ar dating method. *Journal of Volcanology and Geothermal Research* **133**, 157–170. [https://doi.org/10.1016/S0377-0273\(03\)00396-2](https://doi.org/10.1016/S0377-0273(03)00396-2).
- Del Moro, A., Fulignati, P., Marianelli, P. & Sbrana, A. (2001). Magma contamination by direct wall rock interaction: constraints from xenoliths from the walls of a carbonate-hosted magma chamber (Vesuvius 1944 eruption). *Journal of Volcanology and Geothermal Research* **112**, 15–24. [https://doi.org/10.1016/S0377-0273\(01\)00231-1](https://doi.org/10.1016/S0377-0273(01)00231-1).
- Di Fiore, F., Mollo, S., Vona, A., MacDonald, A., Ubide, T., Nazzari, M., Romano, C. & Scarlato, P. (2021). Kinetic partitioning of major and trace cations between clinopyroxene and phonotephritic melt under convective stirring conditions: new insights into clinopyroxene sector zoning and concentric zoning. *Chemical Geology* **584**, 120531. <https://doi.org/10.1016/j.chemgeo.2021.120531>.
- Di Girolamo, P., Ghiara, M. R., Lirer, L., Munno, R., Rolandi, G. & Stanzione, D. (1984). Vulcanologia e petrologia Dei Campi Flegrei. *Italian Journal of Geosciences* **103**, 349–413.
- Di Renzo, V., Arienzo, I., Civetta, L., D'Antonio, M., Tonarini, S., Di Vito, M. & Orsi, G. (2011). The magmatic feeding system of the Campi Flegrei caldera: architecture and temporal evolution. *Chemical Geology* **281**, 227–241. <https://doi.org/10.1016/j.chemgeo.2010.12.010>.
- Di Vito, M., Isaia, R., Orsi, G., Southon, J. D., De Vita, S., d'Antonio, M., Pappalardo, L. & Piochi, M. (1999). Volcanism and deformation since 12,000 years at the Campi Flegrei caldera (Italy). *Journal of Volcanology and Geothermal Research* **91**, 221–246. [https://doi.org/10.1016/S0377-0273\(99\)00037-2](https://doi.org/10.1016/S0377-0273(99)00037-2).
- Di Vito, M., Sulpizio, R., Zanchetta, G. & D'Orazio, M. (2008). The late Pleistocene pyroclastic deposits of the Campanian plain: new insights into the explosive activity of Neapolitan volcanoes. *Journal of Volcanology and Geothermal Research* **177**, 19–48. <https://doi.org/10.1016/j.jvolgeores.2007.11.019>.
- Edmonds, M., Cashman, K. V., Holness, M. & Jackson, M. (2019). Architecture and dynamics of magma reservoirs. *Philos Trans A Math Phys Eng Sci* **377**, 20180298. <https://doi.org/10.1098/rsta.2018.0298>.
- Egglar, D. H. (1972). Water-saturated and undersaturated melting relations in a Paricutin andesite and an estimate of water content in the natural magma. *Contributions to Mineralogy and Petrology* **34**, 261–271. <https://doi.org/10.1007/BF00373757>.
- Fabbrizio, A., & Carroll, M. R. (2008). Experimental constraints on the differentiation process and pre-eruptive conditions in the magmatic system of Phlegraean Fields (Naples, Italy). *Journal of Volcanology and Geothermal Research* **171**(1-2), 88–102. <https://doi.org/10.1016/j.jvolgeores.2007.11.002>.
- Faccenna, C., Funicello, F., Civetta, L., D'Antonio, M., Moroni, M. & Piromallo, C. (2007) Slab disruption, mantle circulation, and the

- opening of the Tyrrhenian basins. In: Beccaluva L., Bianchini G. & Wilson M. (eds) *Cenozoic Volcanism in the Mediterranean Area*. Boulder, Colorado: Geological Society of America, pp.153–169.
- Fedele, L., Tarzia, M., Belkin, H. E., De Vivo, B., Lima, A. & Lowenstern, J. B. (2006) Magmatic-hydrothermal fluid interaction and mineralization in alkali-syenite nodules from the Breccia Museo pyroclastic deposit, Naples, Italy. In: Vivo, B. D. (ed.) *Developments in Volcanology*. Amsterdam: Elsevier, pp.125–161.
- Fedele, L., Scarpato, C., Lanphere, M., Melluso, L., Morra, V., Perrotta, A. & Ricci, G. (2008). The breccia Museo formation, Campi Flegrei, southern Italy: geochronology, chemostratigraphy and relationship with the Campanian ignimbrite eruption. *Bulletin of Volcanology* **70**, 1189–1219. <https://doi.org/10.1007/s00445-008-0197-y>.
- Feig, S. T., Koepke, J. & Snow, J. E. (2010). Effect of oxygen fugacity and water on phase equilibria of a hydrous tholeiitic basalt. *Contributions to Mineralogy and Petrology* **160**, 551–568. <https://doi.org/10.1007/s00410-010-0493-3>.
- Fernandez, G., Giaccio, B., Costa, A., Monaco, L., Nomade, S., Albert, P. G., Pereira, A., Flynn, M., Leicher, N., Lucchi, F., Petrosino, P., Palladino, D. M., Milia, A., Insinga, D. D., Wulf, S., Kearney, R., Veres, D., Jordanova, D., Putignano, M. L., Isaia, R. & Sottili, G. (2024). New constraints on the middle-Late Pleistocene Campi Flegrei explosive activity and Mediterranean tephrostratigraphy (~160 ka and 110–90 ka). *Quaternary Science Reviews* **331**, 108623. <https://doi.org/10.1016/j.quascirev.2024.108623>.
- Ferrucci, F., Gaudiosi, G., Pino, N. A., Luongo, G., Hirn, A. & Mirabile, L. (1989). Seismic detection of a major Moho upheaval beneath the Campania volcanic area (Naples, southern Italy). *Geophysical Research Letters* **16**, 1317–1320. <https://doi.org/10.1029/GL016i011.p01317>.
- Filice, F., Liberi, F., Cirillo, D., Pandolfi, L., Marroni, M. & Piluso, E. (2015). Geology map of the central area of catena Costiera: insights into the tectono-metamorphic evolution of the Alpine belt in northern Calabria. *Journal of Maps* **11**, 114–125. <https://doi.org/10.1080/17445647.2014.944877>.
- Fisk, M. R. & Bence, A. E. (1980). Experimental crystallization of chrome spinel in FAMOUS basalt 527-1-1. *Earth and Planetary Science Letters* **48**, 111–123. [https://doi.org/10.1016/0012-821X\(80\)90174-0](https://doi.org/10.1016/0012-821X(80)90174-0).
- Forni, F., Bachmann, O., Mollo, S., De Astis, G., Gelman, S. E. & Ellis, B. S. (2016). The origin of a zoned ignimbrite: insights into the Campanian ignimbrite magma chamber (Campi Flegrei, Italy). *Earth and Planetary Science Letters* **449**, 259–271. <https://doi.org/10.1016/j.epsl.2016.06.003>.
- Forni, F., Degruyter, W., Bachmann, O., De Astis, G. & Mollo, S. (2018). Long-term magmatic evolution reveals the beginning of a new caldera cycle at Campi Flegrei. *Science Advances* **4**, eaat9401. <https://doi.org/10.1126/sciadv.aat9401>.
- Fourmentraux, C., Métrich, N., Bertagnini, A. & Rosi, M. (2012). Crystal fractionation, magma step ascent, and syn-eruptive mingling: the Averno 2 eruption (Phlegraean fields, Italy). *Contributions to Mineralogy and Petrology* **163**, 1121–1137. <https://doi.org/10.1007/s00410-012-0720-1>.
- Fowler, S. J. & Spera, F. J. (2010). A metamodel for crustal magmatism: phase equilibria of giant ignimbrites. *Journal of Petrology* **51**, 1783–1830. <https://doi.org/10.1093/petrology/egq039>.
- Fowler, S. J., Spera, F. J., Bohron, W. A., Belkin, H. E. & De Vivo, B. (2007). Phase equilibria constraints on the chemical and physical evolution of the Campanian ignimbrite. *Journal of Petrology* **48**, 459–493. <https://doi.org/10.1093/petrology/egl068>.
- Fred, R., Heinonen, J. S., Heinonen, A. & Bohron, W. A. (2022). Thermodynamic constraints on the petrogenesis of massif-type anorthosites and their parental magmas. *Lithos* **422–423**, 106751. <https://doi.org/10.1016/j.lithos.2022.106751>.
- Frost, B. R. (1991). Introduction to oxygen fugacity and its petrologic importance. *Reviews in Mineralogy and Geochemistry* **25**, 1–9. <https://doi.org/10.1515/9781501508684-004>.
- Fulginiti, P., Marianelli, P., Santacroce, R. & Sbrana, A. (2000). The skarn shell of the 1944 Vesuvius magma chamber. Genesis and P-T-X conditions from melt and fluid inclusion data. *European Journal of Mineralogy* **12**, 1025–1039. <https://doi.org/10.1127/0935-1221/2000/0012-1025>.
- Gaetani, G. A., Grove, T. L. & Bryan, W. B. (1993). The influence of water on the petrogenesis of subduction-related igneous rocks. *Nature* **365**, 332–334. <https://doi.org/10.1038/365332a0>.
- Gainsforth, Z., Butterworth, A. L., Stodolna, J., Westphal, A. J., Huss, G. R., Nagashima, K., Ogiore, R., Brownlee, D. E., Joswiak, D., Tylliszczak, T. & Simionovici, A. S. (2015). Constraints on the formation environment of two chondrule-like igneous particles from comet 81P/wild 2. *Meteoritics & Planetary Science* **50**, 976–1004. <https://doi.org/10.1111/maps.12445>.
- Gardner, J. E., Befus, K. S., Gualda, G. A. & Ghiorso, M. S. (2014). Experimental constraints on rhyolite-MELTS and the late bishop tuff magma body. *Contributions to Mineralogy and Petrology* **168**, 1–14. <https://doi.org/10.1007/s00410-014-1051-1>.
- Gebauer, S. K., Schmitt, A. K., Pappalardo, L., Stockli, D. F. & Lovera, O. M. (2014). Crystallization and eruption ages of breccia Museo (Campi Flegrei caldera, Italy) plutonic clasts and their relation to the Campanian ignimbrite. *Contributions to Mineralogy and Petrology* **167**, 1–18. <https://doi.org/10.1007/s00410-013-0953-7>.
- Ghiorso, M. S. & Gualda, G. A. (2015). An H₂O–CO₂ mixed fluid saturation model compatible with rhyolite-MELTS. *Contributions to Mineralogy and Petrology* **169**, 1–30.
- Ghiorso, M. S. & Kelemen, P. B. (1987). Evaluating reaction stoichiometry in magmatic systems evolving under generalized thermodynamic constraints: examples comparing isothermal and isenthalpic assimilation. *Magmatic Processes: Physicochemical Principles* **1**, 319–336.
- Ghiorso, M. S. & Sack, R. O. (1995). Chemical mass transfer in magmatic processes IV. A revised and internally consistent thermodynamic model for the interpolation and extrapolation of liquid–solid equilibria in magmatic systems at elevated temperatures and pressures. *Contributions to Mineralogy and Petrology* **199**, 197–212.
- Giaccio, B., Hajdas, I., Isaia, R., Deino, A. & Nomade, S. (2017). High-precision ¹⁴C and ⁴⁰Ar/³⁹Ar dating of the Campanian ignimbrite (Y-5) reconciles the time-scales of climatic-cultural processes at 40 ka. *Scientific Reports* **7**, 1–10. <https://doi.org/10.1038/srep45940>.
- Giacomuzzi, G., Chiarabba, C., Bianco, F., De Gori, P. & Agostinetti, N. P. (2024). Tracking transient changes in the plumbing system at Campi Flegrei caldera. *Earth and Planetary Science Letters* **637**, 118744. <https://doi.org/10.1016/j.epsl.2024.118744>.
- Gibson, S. A., Geist, D. G., Day, J. A. & Dale, C. W. (2012). Short wavelength heterogeneity in the Galápagos plume: evidence from compositionally diverse basalts on Isla Santiago. *Geochemistry, Geophysics, Geosystems* **13**. <https://doi.org/10.1029/2012GC004244>.
- Gilg, H. A., Lima, A., Somma, R., Belkin, H. E. & Ayuso, R. A. (2001). Isotope geochemistry and fluid inclusion study of skarns from Vesuvius. *Mineralogy and Petrology* **73**, 145–176. <https://doi.org/10.1007/s007100170015>.
- Giordano, G. & Caricchi, L. (2022). Determining the state of activity of Transcrustal magmatic systems and their volcanoes. *Annual Review of Earth and Planetary Sciences* **50**, 231–259. <https://doi.org/10.1146/annurev-earth-032320-084733>.

- Gleeson, M. L., Stock, M. J., Pyle, D. M., Mather, T. A., Hutchison, W., Yirgu, G. & Wade, J. (2017). Constraining magma storage conditions at a restless volcano in the Main Ethiopian rift using phase equilibria models. *Journal of Volcanology and Geothermal Research* **337**, 44–61. <https://doi.org/10.1016/j.jvolgeores.2017.02.026>.
- Gleeson, M. L., Antoshechkina, P. M. & Wieser, P. E. (2023). pyMELTScalc - a Python3 package for fast, easy, and flexible MELTS calculations. *AGU Fall Meeting Abstracts*, V53A–V05A.
- Graessner, T. & Schenk, V. (2001). An exposed Hercynian deep crustal section in the Sila massif of northern Calabria: mineral chemistry, petrology and a P-T path of granulite-facies Metapelitic Migmatites and Metabasites. *Journal of Petrology* **42**, 931–961. <https://doi.org/10.1093/ptetrology/42.5.931>.
- Gualda, G. A. R., Ghiorso, M. S., Lemons, R. V. & Carley, T. L. (2012). Rhyolite-MELTS: a modified calibration of MELTS optimized for silica-rich, fluid-bearing magmatic systems. *Journal of Petrology* **53**, 875–890. <https://doi.org/10.1093/ptetrology/egr080>.
- Higgins, O. & Stock, M. J. (2024). A new calibration of the OPAM Thermobarometer for anhydrous and hydrous mafic systems. *Journal of Petrology* **65**, egae043. <https://doi.org/10.1093/ptetrology/egae043>.
- Hill, R. & Roeder, P. (1974). The crystallization of spinel from basaltic liquid as a function of oxygen fugacity. *The Journal of Geology* **82**, 709–729. <https://doi.org/10.1086/628026>.
- Horn, E. L., Taylor, R. N., Gernon, T. M., Stock, M. J. & Farley, E. M. R. (2022). Composition and petrology of a mush-bearing magma reservoir beneath Tenerife. *Journal of Petrology* **63**, egac095. <https://doi.org/10.1093/ptetrology/egac095>.
- Iacono Marziano, G., Gaillard, F. & Pichavant, M. (2008). Limestone assimilation by basaltic magmas: an experimental re-assessment and application to Italian volcanoes. *Contributions to Mineralogy and Petrology* **155**, 719–738. <https://doi.org/10.1007/s00410-007-0267-8>.
- Iovine, R. S., Mazzeo, F. C., Wörner, G., Pelullo, C., Cirillo, G., Arienzo, I., Pack, A., & D'Antonio, M. (2018). Coupled $\delta^{18}\text{O}$ - $\delta^{17}\text{O}$ and $87\text{Sr}/86\text{Sr}$ isotope compositions suggest a radiogenic and ^{18}O -enriched magma source for Neapolitan volcanoes (Southern Italy). *Lithos*, **316-317**, 199–211. <https://doi.org/10.1016/j.lithos.2018.07.009>.
- Isaia, R., D'Antonio, M., Dell'Erba, F., Di Vito, M. & Orsi, G. (2004). The Astroni volcano: the only example of closely spaced eruptions in the same vent area during the recent history of the Campi Flegrei caldera (Italy). *Journal of Volcanology and Geothermal Research* **133**, 171–192. [https://doi.org/10.1016/S0377-0273\(03\)00397-4](https://doi.org/10.1016/S0377-0273(03)00397-4).
- Isaia, R., Marianelli, P. & Sbrana, A. (2009). Caldera unrest prior to intense volcanism in Campi Flegrei (Italy) at 4.0 ka BP: implications for caldera dynamics and future eruptive scenarios. *Geophysical Research Letters* **36**. <https://doi.org/10.1029/2009GL040513>.
- Isaia, R., Vitale, S., Marturano, A., Aiello, G., Barra, D., Ciarcia, S., Iannuzzi, E. & Tramparulo, F. D. (2019). High-resolution geological investigations to reconstruct the long-term ground movements in the last 15 kyr at Campi Flegrei caldera (southern Italy). *Journal of Volcanology and Geothermal Research* **385**, 143–158. <https://doi.org/10.1016/j.jvolgeores.2019.07.012>.
- Isaia, R., Troiano, A., Di Giuseppe, M. G., De Paola, C., Gottsmann, J., Pagliara, F., Smith, V. C. & Stock, M. J. (2025). 3D magnetotelluric imaging of a transcrustal magma system beneath the Campi Flegrei caldera, southern Italy. *Communications Earth & Environment* **6**, 1–16. <https://doi.org/10.1038/s43247-025-02185-5>.
- James, D. E. (1981). The combined use of oxygen and radiogenic isotopes as indicators of crustal contamination. *Annual Review of Earth and Planetary Sciences* **9**, 311–344. <https://doi.org/10.1146/annurev.ea.09.050181.001523>.
- Jochum, K. P., Stoll, B., Herwig, K., Willbold, M., Hofmann, A. W., Amini, M., Aarburg, S., Abouchami, W., Hellebrand, E., Mocek, B., Raczek, I., Stracke, A., Alard, O., Bouman, C., Becker, S., Dücking, M., Brätz, H., Klemd, R., de Bruin, D., Canil, D., Cornell, D., de Hoog, C. J., Dalpé, C., Danyushevsky, L., Eisenhauer, A., Gao, Y., Snow, J. E., Groschopf, N., Günther, D., Latkoczy, C., Guillong, M., Hauri, E. H., Höfer, H. E., Lahaye, Y., Horz, K., Jacob, D. E., Kasemann, S. A., Kent, A. J. R., Ludwig, T., Zack, T., Mason, P. R. D., Meixner, A., Rosner, M., Misawa, K., Nash, B. P., Pfänder, J., Premo, W. R., Sun, W. D., Tiepolo, M., Vannucci, R., Vennemann, T., Wayne, D. & Woodhead, J. D. (2006). MPI-DING reference glasses for in situ microanalysis: new reference values for element concentrations and isotope ratios. *Geochemistry, Geophysics, Geosystems* **7**. <https://doi.org/10.1029/2005GC001060>.
- Judenherc, S. & Zollo, A. (2004). The bay of Naples (southern Italy): constraints on the volcanic structures inferred from a dense seismic survey. *Journal of Geophysical Research: Solid Earth* **109**. <https://doi.org/10.1029/2003JB002876>.
- Kelemen, P., Yogodzinski, G. & Scholl, D. W. (2003). Along-strike variation in lavas of the Aleutian island arc: implications for the genesis of high-Mg# andesite and the continental crust. *American Geophysical Union. Geophysical Monograph* **138**, 223–274.
- Kent, A. J., Blundy, J., Cashman, K. V., Cooper, K. M., Donnelly, C., Pallister, J. S., Reagan, M., Rowe, M. C. & Thornber, C. R. (2007). Vapor transfer prior to the October 2004 eruption of Mount St. Helens, Washington. *Geology* **35**, 231–234. <https://doi.org/10.1130/G22809A.1>.
- Knafelc, J., Bryan, S. E., Gust, D. & Cathey, H. E. (2020). Defining pre-eruptive conditions of the Havre 2012 submarine rhyolite eruption using crystal archives. *Frontiers in Earth Science* **8**. <https://doi.org/10.3389/feart.2020.00310>.
- Kress, V. C. & Ghiorso, M. S. (2004). Thermodynamic modeling of post-entrapment crystallization in igneous phases. *Journal of Volcanology and Geothermal Research* **137**, 247–260. <https://doi.org/10.1016/j.jvolgeores.2004.05.012>.
- Landi, P., Métrich, N., Bertagnini, A. & Rosi, M. (2004). Dynamics of magma mixing and degassing recorded in plagioclase at Stromboli (Aeolian archipelago, Italy). *Contributions to Mineralogy and Petrology* **147**, 213–227. <https://doi.org/10.1007/s00410-004-0555-5>.
- Lange, R. A., Frey, H. M. & Hector, J. (2009). A thermodynamic model for the plagioclase-liquid hygrometer/thermometer. *American Mineralogist* **94**, 494–506. <https://doi.org/10.2138/am.2009.3011>.
- Lipman, P. W. (1984). The roots of ash flow calderas in western North America: windows into the tops of granitic batholiths. *Journal of Geophysical Research: Solid Earth* **89**, 8801–8841. <https://doi.org/10.1029/JB089iB10p08801>.
- Lowenstern, J. (1995). Applications of silicate melt inclusions to the study of magmatic volatiles. *Chemical Geology* **183**, 5–24.
- Mangiacapra, A., Moretti, R., Rutherford, M., Civetta, L., Orsi, G. & Papale, P. (2008). The deep magmatic system of the Campi Flegrei caldera (Italy). *Geophysical Research Letters* **35**. <https://doi.org/10.1029/2008GL035550>.
- Masotta, M., Mollo, S., Freda, C., Gaeta, M. & Moore, G. (2013). Clinopyroxene-liquid thermometers and barometers specific to alkaline differentiated magmas. *Contributions to Mineralogy and Petrology* **166**, 1545–1561. <https://doi.org/10.1007/s00410-013-0927-9>.
- Mazzeo, F. C., D'Antonio, M., Arienzo, I., Aulinas, M., Di Renzo, V. & Gimeno, D. (2014). Subduction-related enrichment of the Neapolitan volcanoes (southern Italy) mantle source: new constraints on the characteristics of the slab-derived components. *Chemical Geology* **386**, 165–183. <https://doi.org/10.1016/j.chemgeo.2014.08.014>.

- Natale, J., Camanni, G., Ferranti, L., Isaia, R., Sacchi, M., Spiess, V., Steinmann, L. & Vitale, S. (2022a). Fault systems in the offshore sector of the Campi Flegrei caldera (southern Italy): implications for nested caldera structure, resurgent dome, and volcano-tectonic evolution. *Journal of Structural Geology* **163**, 104723. <https://doi.org/10.1016/j.jsg.2022.104723>.
- Natale, J., Ferranti, L., Isaia, R., Marino, C., Sacchi, M., Spiess, V., Steinmann, L. & Vitale, S. (2022b). Integrated on-land-offshore stratigraphy of the Campi Flegrei caldera: new insights into the volcano-tectonic evolution in the last 15 kyr. *Basin Research* **34**, 855–882. <https://doi.org/10.1111/bre.12643>.
- Natale, J., Vitale, S. & Isaia, R. (2024a). Simultaneous normal and reverse faulting in reactivating caldera faults: a detailed field structural analysis from Campi Flegrei (southern Italy). *Journal of Structural Geology* **181**, 105109. <https://doi.org/10.1016/j.jsg.2024.105109>.
- Natale, J., Vitale, S., Repola, L., Monti, L. & Isaia, R. (2024b). Geomorphic analysis of digital elevation model generated from vintage aerial photographs: a glance at the pre-urbanization morphology of the active Campi Flegrei caldera. *Geomorphology* **460**, 109267. <https://doi.org/10.1016/j.geomorph.2024.109267>.
- Németh, K., Carrasco-Núñez, G., Aranda-Gómez, J. J. & Smith, I. E. M. (2017) *Monogenetic Volcanism*. London: Geological Society of London.
- Nunziata, C. (2010). Low shear-velocity zone in the Neapolitan-area crust between the Campi Flegrei and Vesuvio volcanic areas. *Terra Nova* **22**, 208–217. <https://doi.org/10.1111/j.1365-3121.2010.00936.x>.
- Orsi, G., De Vita, S. & Di Vito, M. (1996). The restless, resurgent Campi Flegrei nested caldera (Italy): constraints on its evolution and configuration. *Journal of Volcanology and Geothermal Research* **74**, 179–214. [https://doi.org/10.1016/S0377-0273\(96\)00063-7](https://doi.org/10.1016/S0377-0273(96)00063-7).
- Orsi, G., Di Vito, M. A. & Isaia, R. (2004). Volcanic hazard assessment at the restless Campi Flegrei caldera. *Bulletin of Volcanology* **66**, 514–530. <https://doi.org/10.1007/s00445-003-0336-4>.
- Pamukcu, A. S., Gualda, G. A. R., Ghiorso, M. S., Miller, C. F. & McCracken, R. G. (2015). Phase-equilibrium geobarometers for silicic rocks based on rhyolite-MELTS—part 3: application to the peach spring tuff (Arizona–California–Nevada, USA). *Contributions to Mineralogy and Petrology* **169**, 33. <https://doi.org/10.1007/s00410-015-1122-y>.
- Pappalardo, L. & Mastrolorenzo, G. (2012). Rapid differentiation in a sill-like magma reservoir: a case study from the campi flegrei caldera. *Scientific Reports* **2**, 712. <https://doi.org/10.1038/srep00712>.
- Pappalardo, L., Piochi, M., d'Antonio, M., Civetta, L. & Petrini, R. (2002). Evidence for multi-stage magmatic evolution during the past 60 kyr at Campi Flegrei (Italy) deduced from Sr, Nd and Pb isotope data. *Journal of Petrology* **43**, 1415–1434. <https://doi.org/10.1093/ptrology/43.8.1415>.
- Passmore, E., MacLennan, J., Fitton, G. & Thordarson, T. (2012). Mush disaggregation in basaltic magma chambers: evidence from the ad 1783 Laki eruption. *Journal of Petrology* **53**, 2593–2623. <https://doi.org/10.1093/ptrology/egs061>.
- Pearce, J. A. & Peate, D. W. (1995). Tectonic implications of the composition of volcanic arc magmas. *Annual Review of Earth and Planetary Sciences* **23**, 251–285. <https://doi.org/10.1146/annurev.ea.23.050195.001343>.
- Peccerillo, A. (2017) The Campania Province. In: Peccerillo A. (ed) *Cenozoic Volcanism in the Tyrrhenian Sea Region*. Cham: Springer International Publishing, pp.159–201.
- Peccerillo, A. & Frezzotti, M. (2015). Magmatism, mantle evolution and geodynamics at the converging plate margins of Italy. *Journal of the Geological Society* **172**, 407–427. <https://doi.org/10.1144/jgs2014-085>.
- Pérez-Orozco, J. D., Sosa-Ceballos, G. & Macías, J. L. (2021). Tectonic and magmatic controls on the evolution of post-collapse volcanism. Insights from the Acoculco caldera complex, Puebla, México. *Lithos* **380–381**, 105878.
- Perinelli, C., Gaeta, Bonechi Barbara, F., Granati, Carmela, F., Massimo, D., Vincenzo, S., Stefania, S. & Claudia, R. (2019). Effect of water on the phase relations of primitive K-basalts: implications for high-pressure differentiation in the Phlegraean Volcanic District magmatic system. *Lithos* **342–343**, 530–541.
- Petrelli, M., Ágreda López, M., Pisello, A. & Perugini, D. (2023). Pre-eruptive dynamics at the Campi Flegrei caldera: from evidence of magma mixing to timescales estimates. *Earth, Planets and Space* **75**, 19. <https://doi.org/10.1186/s40623-023-01765-z>.
- Piochi, M., Mastrolorenzo, G. & Pappalardo, L. (2005). Magma ascent and eruptive processes from textural and compositional features of Monte Nuovo pyroclastic products, Campi Flegrei, Italy. *Bulletin of Volcanology* **67**, 663–678. <https://doi.org/10.1007/s00445-005-0410-1>.
- Piochi, M., Polacci, M., De Astis, G., Zanetti, A., Mangiacapra, A., Vannucci, R. & Giordano, D. (2008). Texture and composition of pumices and scoriae from the Campi Flegrei caldera (Italy): implications on the dynamics of explosive eruptions. *Geochemistry, Geophysics, Geosystems* **9**. <https://doi.org/10.1029/2007GC001746>.
- Piochi, M., Kilburn, C. R. J., Di Vito, M. A., Mormone, A., Tramelli, A., Troise, C. & De Natale, G. (2014). The volcanic and geothermally active Campi Flegrei caldera: an integrated multidisciplinary image of its buried structure. *International Journal of Earth Sciences* **103**, 401–421. <https://doi.org/10.1007/s00531-013-0972-7>.
- Pistolesi, M., Bertagnini, A., Di Roberto, A., Isaia, R., Vona, A., Cioni, R. & Giordano, G. (2017). The Baia-Fondi di Baia eruption at Campi Flegrei: stratigraphy and dynamics of a multi-stage caldera reactivation event. *Bulletin of Volcanology* **79**, 67. <https://doi.org/10.1007/s00445-017-1149-1>.
- Pontevivo, A. & Panza, G. F. (2006). The lithosphere-asthenosphere system in the Calabrian arc and surrounding seas – southern Italy. *Pure and Applied Geophysics* **163**, 1617–1659. <https://doi.org/10.1007/s00024-006-0093-3>.
- Putirka, K. D. (2008). Thermometers and barometers for volcanic systems. *Reviews in Mineralogy and Geochemistry* **69**, 61–120. <https://doi.org/10.2138/rmg.2008.69.3>.
- Robertson, E. A. M., Biggs, J., Cashman, K. V., Floyd, M. A. & Vye-Brown, C. (2016). Influence of regional tectonics and pre-existing structures on the formation of elliptical calderas in the Kenyan rift. *Geological Society, London, Special Publications* **420**, 43–67. <https://doi.org/10.1144/SP420.12>.
- Rolandi, G., Bellucci, F., Heizler, M. T., Belkin, H. E. & De Vivo, B. (2003). Tectonic controls on the genesis of ignimbrites from the Campanian volcanic zone, southern Italy. *Mineralogy and Petrology* **79**, 3–31. <https://doi.org/10.1007/s00710-003-0014-4>.
- Romano, C., Giordano, D., Papale, P., Mincione, V., Dingwell, D. B. & Rosi, M. (2003). The dry and hydrous viscosities of alkaline melts from Vesuvius and Phlegrean fields. *Chemical Geology* **202**, 23–38. [https://doi.org/10.1016/S0009-2541\(03\)00208-0](https://doi.org/10.1016/S0009-2541(03)00208-0).
- Rooney, T. O., Hart, W. K., Hall, C. M., Ayalew, D., Ghiorso, M. S., Hidalgo, P. & Yirgu, G. (2012). Peralkaline magma evolution and the tephra record in the Ethiopian rift. *Contributions to Mineralogy and Petrology* **164**, 407–426. <https://doi.org/10.1007/s00410-012-0744-6>.
- Rosi, M. & Sbrana, A. (1987). Phlegrean fields. *Quaderni de la ricerca scientifica* **9**.

- Sarbas, B. (2008). The GEOROC database as part of a growing geoinformatics network. paper presented at the Geoinformatics 2008—Data to Knowledge. USGS, 42–43.
- Saxby, J., Gottsmann, J., Cashman, K. & Gutiérrez, E. (2016). Magma storage in a strike-slip caldera. *Nature Communications* **7**, 12295. <https://doi.org/10.1038/ncomms12295>.
- Scandone, R., Bellucci, F., Lirer, L. & Rolandi, G. (1991). The structure of the Campanian plain and the activity of the Neapolitan volcanoes (Italy). *Journal of Volcanology and Geothermal Research* **48**, 1–31. [https://doi.org/10.1016/0377-0273\(91\)90030-4](https://doi.org/10.1016/0377-0273(91)90030-4).
- Scotto di Uccio, F., Lomax, A., Natale, J., Muzellec, T., Festa, G., Nazeri, S., Convertito, V., Bobbio, A., Strumia, C. & Zollo, A. (2024). Delineation and fine-scale structure of fault zones activated during the 2014–2024 unrest at the Campi Flegrei caldera (southern Italy) from high-precision earthquake locations. *Geophysical Research Letters* **51**, e2023GL107680. <https://doi.org/10.1029/2023GL107680>.
- Sims, K. W. W., MacLennan, J., Blichert-Toft, J., Mervine, E. M., Blusztajn, J. & Grönvold, K. (2013). Short length scale mantle heterogeneity beneath Iceland probed by glacial modulation of melting. *Earth and Planetary Science Letters* **379**, 146–157. <https://doi.org/10.1016/j.epsl.2013.07.027>.
- Sisson, T. W. & Grove, T. L. (1993). Experimental investigations of the role of H₂O in calc-alkaline differentiation and subduction zone magmatism. *Contributions to Mineralogy and Petrology* **113**, 143–166. <https://doi.org/10.1007/BF00283225>.
- Smith, P. M. & Asimow, P. D. (2005). *Adiabat_1ph*: a new public front-end to the MELTS, pMELTS, and pHMELTS models. *Geochemistry, Geophysics, Geosystems* **6**. <https://doi.org/10.1029/2004GC000816>.
- Smith, V., Isaia, R. & Pearce, N. (2011). Tephrostratigraphy and glass compositions of post-15 kyr Campi Flegrei eruptions: implications for eruption history and chronostratigraphic markers. *Quaternary Science Reviews* **30**, 3638–3660. <https://doi.org/10.1016/j.quascirev.2011.07.012>.
- Sollevanti, F. (1983). Geologic, volcanologic, and tectonic setting of the Vico-Cimino area, Italy. *Journal of Volcanology and Geothermal Research* **17**, 203–217. [https://doi.org/10.1016/0377-0273\(83\)90068-9](https://doi.org/10.1016/0377-0273(83)90068-9).
- Stock, M. J., Humphreys, M. C., Smith, V. C., Isaia, R. & Pyle, D. M. (2016). Late-stage volatile saturation as a potential trigger for explosive volcanic eruptions. *Nature Geoscience* **9**, 249–254. <https://doi.org/10.1038/ngeo2639>.
- Stock, M. J., Humphreys, M. C., Smith, V. C., Isaia, R., Brooker, R. A. & Pyle, D. M. (2018). Tracking volatile behaviour in sub-volcanic plumbing systems using apatite and glass: insights into pre-eruptive processes at Campi Flegrei, Italy. *Journal of Petrology* **59**, 2463–2492. <https://doi.org/10.1093/petrology/egy020>.
- Tomlinson, E. L., Arienzo, I., Civetta, L., Wulf, S., Smith, V. C., Hardiman, M., Lane, C. S., Carandente, A., Orsi, G., Rosi, M., Müller, W. & Menzies, M. A. (2012). Geochemistry of the Phlegraean fields (Italy) proximal sources for major Mediterranean tephras: implications for the dispersal of Plinian and co-ignimbritic components of explosive eruptions. *Geochimica et Cosmochimica Acta* **93**, 102–128. <https://doi.org/10.1016/j.gca.2012.05.043>.
- Toplis, M. J. & Carroll, M. R. (1995). An experimental study of the influence of oxygen fugacity on Fe-Ti oxide stability, phase relations, and mineral–melt equilibria in Ferro-basaltic systems. *Journal of Petrology* **36**, 1137–1170. <https://doi.org/10.1093/petrology/36.5.1137>.
- Troiano, A., Di Giuseppe, M. G., Petrillo, Z., Troise, C. & De Natale, G. (2011). Ground deformation at calderas driven by fluid injection: modelling unrest episodes at Campi Flegrei (Italy). *Geophysical Journal International* **187**, 833–847. <https://doi.org/10.1111/j.1365-246X.2011.05149.x>.
- Troiano, A., Di Giuseppe, M. G. & Isaia, R. (2022). 3D structure of the Campi Flegrei caldera central sector reconstructed through short-period magnetotelluric imaging. *Scientific Reports* **12**, 20802. <https://doi.org/10.1038/s41598-022-24998-6>.
- Vetere, F., Botcharnikov, R. E., Holtz, F., Behrens, H. & De Rosa, R. (2011). Solubility of H₂O and CO₂ in shoshonitic melts at 1250 C and pressures from 50 to 400 MPa: implications for Campi Flegrei magmatic systems. *Journal of Volcanology and Geothermal Research* **202**, 251–261. <https://doi.org/10.1016/j.jvolgeores.2011.03.002>.
- Vilardo, G., Isaia, R., Ventura, G., De Martino, P. & Terranova, C. (2010). InSAR permanent Scatterer analysis reveals fault reactivation during inflation and deflation episodes at Campi Flegrei caldera. *Remote Sensing of Environment* **114**, 2373–2383. <https://doi.org/10.1016/j.rse.2010.05.014>.
- Villemant, B. (1988). Trace element evolution in the Phlegraean fields (Central Italy): fractional crystallization and selective enrichment. *Contributions to Mineralogy and Petrology* **98**, 169–183. <https://doi.org/10.1007/BF00402110>.
- Vineberg, S. O., Isaia, R., Albert, P. G., Brown, R. J. & Smith, V. C. (2023). Insights into the explosive eruption history of the Campanian volcanoes prior to the Campanian ignimbrite eruption. *Journal of Volcanology and Geothermal Research* **443**, 107915. <https://doi.org/10.1016/j.jvolgeores.2023.107915>.
- de Vita, S., Orsi, G., Civetta, L., Carandente, A., D'Antonio, M., Deino, A., di Cesare, T., di Vito, M. A., Fisher, R. V., Isaia, R., Marotta, E., Necco, A., Ort, M., Pappalardo, L., Piochi, M. & Southon, J. (1999). The Agnano–Monte Spina eruption (4100 years BP) in the restless Campi Flegrei caldera (Italy). *Journal of Volcanology and Geothermal Research* **91**, 269–301. [https://doi.org/10.1016/S0377-0273\(99\)00039-6](https://doi.org/10.1016/S0377-0273(99)00039-6).
- Vitale, S. & Ciarcia, S. (2018). Tectono-stratigraphic setting of the Campania region (southern Italy). *Journal of Maps* **14**, 9–21. <https://doi.org/10.1080/17445647.2018.1424655>.
- Vitale, S. & Isaia, R. (2014). Fractures and faults in volcanic rocks (Campi Flegrei, southern Italy): insight into volcano-tectonic processes. *International Journal of Earth Sciences* **103**, 801–819. <https://doi.org/10.1007/s00531-013-0979-0>.
- Vitale, S. & Natale, J. (2023). Combined volcano-tectonic processes for the drowning of the Roman western coastal settlements at Campi Flegrei (southern Italy). *Earth, Planets and Space* **75**, 38. <https://doi.org/10.1186/s40623-023-01795-7>.
- Voloschina, M., Pistolesi, M., Bertagnini, A., Métrich, N., Pompilio, M., di Roberto, A., di Salvo, S., Francalanci, L., Isaia, R., Cioni, R. & Romano, C. (2018). Magmatic reactivation of the Campi Flegrei volcanic system: insights from the Baia–Fondi di Baia eruption. *Bulletin of Volcanology* **80**, 75. <https://doi.org/10.1007/s00445-018-1247-8>.
- Webster, J., Raia, F., Tappen, C. & De Vivo, B. (2003). Pre-eruptive geochemistry of the ignimbrite-forming magmas of the Campanian volcanic zone, southern Italy, determined from silicate melt inclusions. *Mineralogy and Petrology* **79**, 99–125. <https://doi.org/10.1007/s00710-003-0004-6>.
- Willmott, C. J. (1981). On the validation of models. *Physical Geography* **2**, 184–194. <https://doi.org/10.1080/02723646.1981.10642213>.
- Woo, J. Y. L. & Kilburn, C. R. J. (2010). Intrusion and deformation at Campi Flegrei, southern Italy: sills, dikes, and regional extension. *Journal of Geophysical Research: Solid Earth* **115**. <https://doi.org/10.1029/2009JB006913>.
- Zollo, A., Maercklin, N., Vassallo, M., Dello Iacono, D., Virieux, J. & Gasparini, P. (2008). Seismic reflections reveal a massive melt layer feeding Campi Flegrei caldera. *Geophysical Research Letters* **35**. <https://doi.org/10.1029/2008GL034242>.